GENERAL ATOMIC

DIVISION OF GENERAL DYNAMICS

GA-4729

PERFORMANCE AND ENERGY TRANSFER MEASUREMENTS ON CYLINDRICAL CESIUM THERMIONIC CONVERTERS

by

J. W. Holland

November 13, 1963

DISCLAIMER

GENERAL ATOMIC

DIVISION OF

GENERAL DYNAMICS

JOHN JAY HOPKINS LABORATORY FOR PURE AND APPLIED SCIENCE

P.O. BOX 608, SAN DIEGO 12, CALIFORNIA

GA-4729

PERFORMANCE AND ENERGY TRANSFER MEASUREMENTS ON CYLINDRICAL CESIUM THERMIONIC CONVERTERS*

Work done by:

F. S. Baker
E. M. Gillette
J. W. Holland
D. E. Schwarzer

Report written by:

J. W. Holland

*This work was supported in part by the U. S. Atomic Energy Commission under Contract AT(04-3)-167, Project Agreement No. 14, and in part under a program of General Atomic and Rocky Mountain–Pacific Nuclear Research Group and San Diego Gas and Electric Company.

November 13, 1963

SUMMARY

Detailed measurements of performance and energy transfer have been made on two highly instrumented cylindrical cesium thermionic converters with electrically heated tungsten emitters. The first converter, OC-4, which had a niobium collector, operated with an initial electrical output of 6.9 watts/cm^2. This output gradually degraded to a value of 4.6 watts/cm^2 after 1351 hr. These power values were measured at the electrodes for an average emitter temperature of 1750°C. Converter OC-5, which had a molybdenum collector, has operated 260 hr to date, with a power output and efficiency of 11.1 watts/cm^2 and 16%, respectively, at an average emitter temperature of 1800°C. These operating data are compared with those for lower emitter temperatures below.

Emitter Temperature (°C)	Power Density (watts/cm^2)	Efficiency (%)
1800	11.1	16
1600	7.5	12
1400	4.2	8.4
1200	1.0	4.9

Energy values of the emitter electron cooling, collector electron heating, thermal radiation, and cesium conduction were calorimetrically determined as a function of emitter temperature, collector temperature, cesium pressure, and current. For all the data obtained, the emitter temperature profile was measured by thermocouples. From the calorimeter measurements, correlations were found for the prediction of emitter electron cooling ΔQ_E and collector electron heating ΔQ_C:

$$\Delta Q_E = I\,(2.6 + V)\ ,$$

$$\Delta Q_C = I\,(2.6)\ .$$

The correlation is valid within 4% accuracy over the operating variable range: emitter temperature of 1200° to 1800°C; cesium reservoir temperature of 300° to 400°C; collector temperature of 600° to 700°C; and current of zero to 15 amp/cm^2. Through measurements of emitter-structure heat losses, of the cesium-vapor thermal conduction, and of the electrode radiation heat transfer, it was found that all the zero-current energy-transfer quantities can be accurately predicted with RAT, a two-dimensional digital-computer heat-transfer code.

The electron cooling correlation, together with the ability to calculate all of the power-loss values in a thermionic converter, makes it possible to compute the efficiency of a converter when the I-V characteristics and materials properties are known. This is of special interest to thermionic reactor analysis, since the input to the reactor problem is the amount of fission produced in each of a very large number of cells within the reactor. Apart from the utility of the correlation discovered, the determination of the value of 2.6 volts in the current-heating terms is of fundamental interest and invites further study.

CONTENTS

I. INTRODUCTION

The first objective of the Mark VI* out-of-pile converter testing program is to obtain bench performance data from the cell which is the counterpart of the in-pile converters, for the diagnosis of any further design, materials, or fabrication problems. Two converters, designated as OC-4 and OC-5, were fabricated and successfully tested to meet this initial objective.

The second objective of the out-of-pile testing program is to precisely determine the thermionic energy-transfer properties of these converters for use in the analysis of thermionic reactor systems employing similar cells. The energy input to converters at zero current can be computed from the properties and geometries of the materials used. At finite currents, however, the emitter power input is a function of the operating variables of emitter temperature, collector temperature, cesium pressure, and current. It becomes one of the primary goals of this work to find correlations for predicting the energy-transfer quantities arising from the conduction of electrical current between the converter electrodes. Although misnamed, these energy quantities are commonly termed "emitter electron cooling" and "collector electron heating."

To obtain these correlation results, experimental techniques have been developed that are more sophisticated than those practiced previously. Experiments were performed for the determination of accurate emitter temperature distribution (Appendix A), and for the measurement of thermal energies received by the collector (Appendix B). The latter experiment was accomplished with a conduction-type calorimeter in which the heat transfer was calculated from the measured temperature gradients. A

*Mark VI is the designation for cylindrical converters designed and built for in-pile and bench tests under AEC Contract AT(04-3)-167.

preliminary experiment was performed on the calorimeter to calibrate the rate of heat conduction.

The energy-transfer measurements and correlations were obtained with both OC-4 and OC-5. However, because a greater number of measurements were made on OC-5 and with greater accuracy, only the OC-5 energy results will be reported herein (Secs. 5.2 and 5.3). The testing procedures for determining the performance and energy data are outlined in Appendix C. A history of the converter operation is given in Appendix D. The reduction of data by a digital-computer code and the instrumentation used are described in Appendixes E and F, respectively.

II. CONVERTER DESIGN

The Mark VI out-of-pile converter and the emitter-temperature-profile and collector-calorimeter instrumentation are shown in Fig. 1. These cylindrical-geometry converters have emitters of vapor-deposited tungsten. Two converters, designated OC-4 and OC-5, were fabricated with the design features listed in Table 1.

Table 1

DESCRIPTION OF TWO MARK VI CONVERTERS

	OC-4	OC-5
Emitter		
Area, cm^2	14.8	14.0
Wall thickness, in.	0.152	0.213
Collector material	Niobium	Molybdenum
Interelectrode spacing (cold), in.	0.011	0.010
Emitter lead		
Material	Tantalum	Tantalum
Area/length	0.0536	0.0787
Interelectrode insulator material	G. E. Lucalox	G. E. Lucalox
Calorimeter material	Niobium	Molybdenum

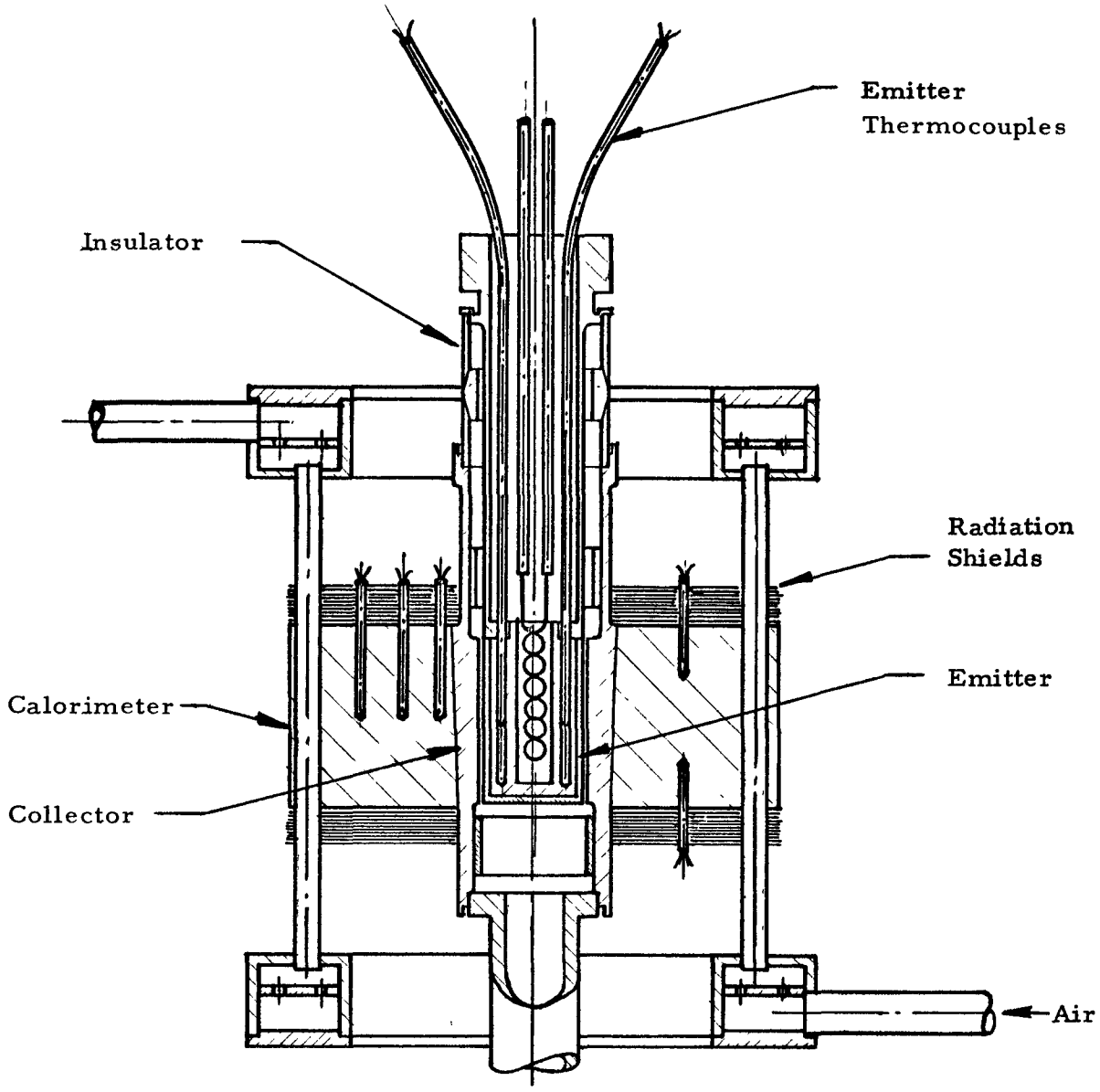

Fig. 1--Design of Mark VI out-of-pile test cells OC-4 and OC-5

Measurement of the emitter temperature profile is made possible through correlations developed in separate experiments that allow the computation of the emitter temperature distribution from the temperatures of four W/W–26 Re thermocouples located in the emitter walls at four axial positions.

The collector calorimeter, as shown in Fig. 1, is a thick-wall cylinder which has located in it many small thermocouples for measuring axial and radial temperature profiles. Ten tantalum radiation heat shields are located at its axial ends to reduce axial heat losses to less than 1 watt. Heat is removed at the outer edge of the calorimeter through 16 closely spaced cooling tubes. A flow of cooling air is uniformly distributed through these tubes by the use of baffled headers. Calrod-type heaters are provided in the outer edge of the calorimeter between the cooling lines for automatic temperature control of the collector.

The total amount of heat removed from the collector is the sum of the heats conducted away in the upper and lower skirts of the collector and the heat conducted through the calorimeter to the cooling lines. Calibration experiments were performed on the calorimeter before the converter was installed, as described in Appendix B. It was determined with the OC-5 calorimeter that the collector heat transfer could be determined to an accuracy of ±35 watts, which results in a 4% error for a total power throughput of 800 watts. Only small errors are introduced in the total collector heat by the uncertainties in the temperature gradients in the collector skirts, since relatively low rates of heat transfer are involved.

III. INITIAL POWER-OPTIMIZATION MEASUREMENTS

Among the initial measurements obtained on these converters are the power-optimization data at emitter temperatures of the order of 1800°C. Optimum values of cell current, cesium-reservoir temperature, and collector temperature are determined while the emitter temperature is maintained constant at a predescribed value. It is important that these

data be obtained as early in the cell life as possible in order to determine if any performance degradation is occurring during the initial hours of operation.

The process of determining the optimum values of the operating variables that give maximum power output is an iterative process because the variables are interdependent. When the final optima are found, curves of the power output versus the variable in question are obtained, as shown in Figs. 2 through 5. These power outputs are obtained at the converter leads. The maximum power produced by OC-4 and OC-5 and the optimum values of the operating variables have been extracted from Figs. 2 through 5 and are listed in Table 2.

Table 2

COMPARISON OF PERFORMANCE OF TWO MARK VI CONVERTERS

	OC-4 (Niobium Collector)	OC-5 (Molybdenum Collector)
Maximum power at converter leads, watts	80	128
Average emitter temperature, °C	1750	1800
Optimized operating variables		
Voltage (lead), volt	0.59	0.67
Current, amp	135	190
Cesium reservoir, °C	350	350
Collector, °C	730	700
Maximum over-all efficiency at emitter leads, %	9.2	13.6

When comparing the outputs of these two converters, the obvious difference is the vastly improved performance of OC-5 over OC-4. The causes for its better performance are believed to be (1) closer hot spacing, (2) more uniform emitter temperature, (3) lower collector work function, (4) no resistive oxide on collector surface,[1] and (5) a 50°C greater emitter

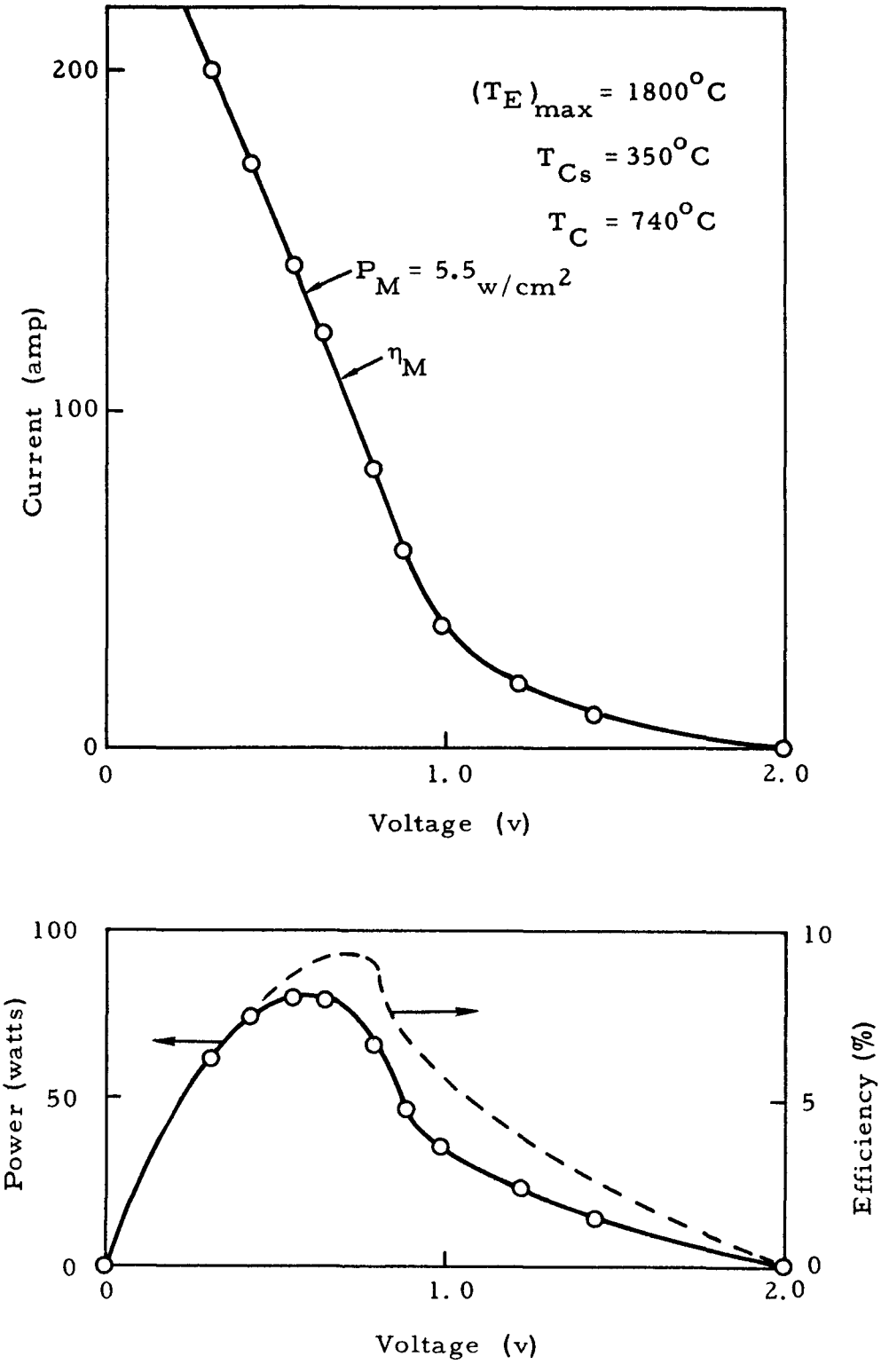

Fig. 2--Initial performance of cell OC-4 (I-V characteristic and optimization of load resistance)

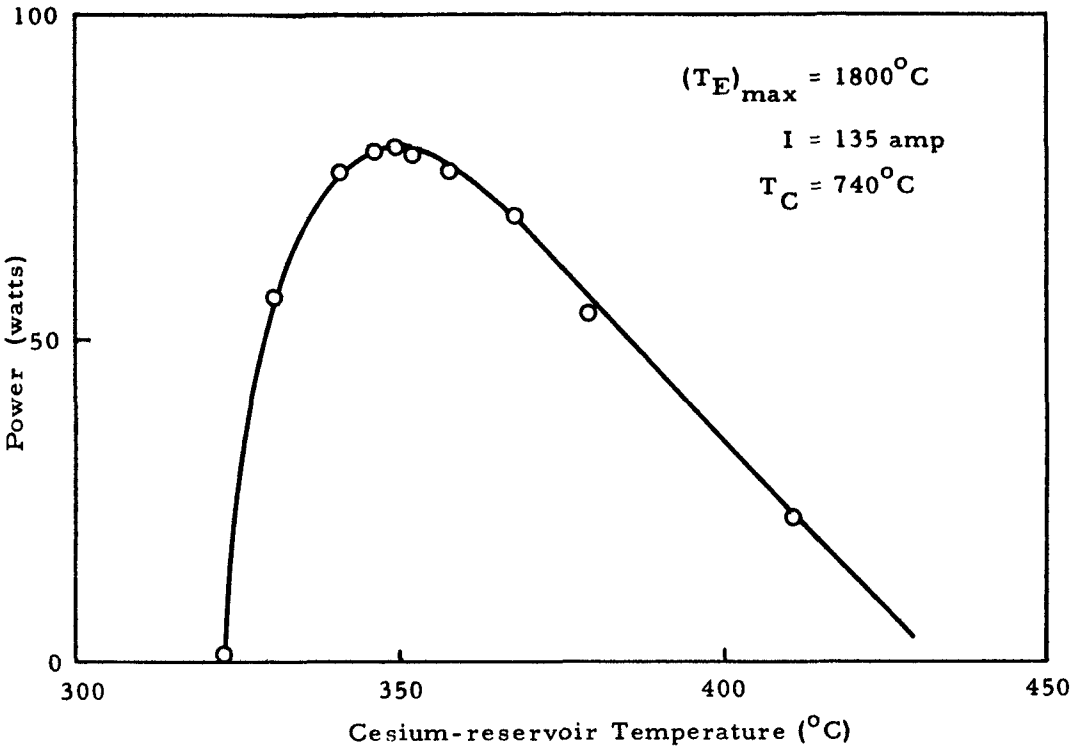

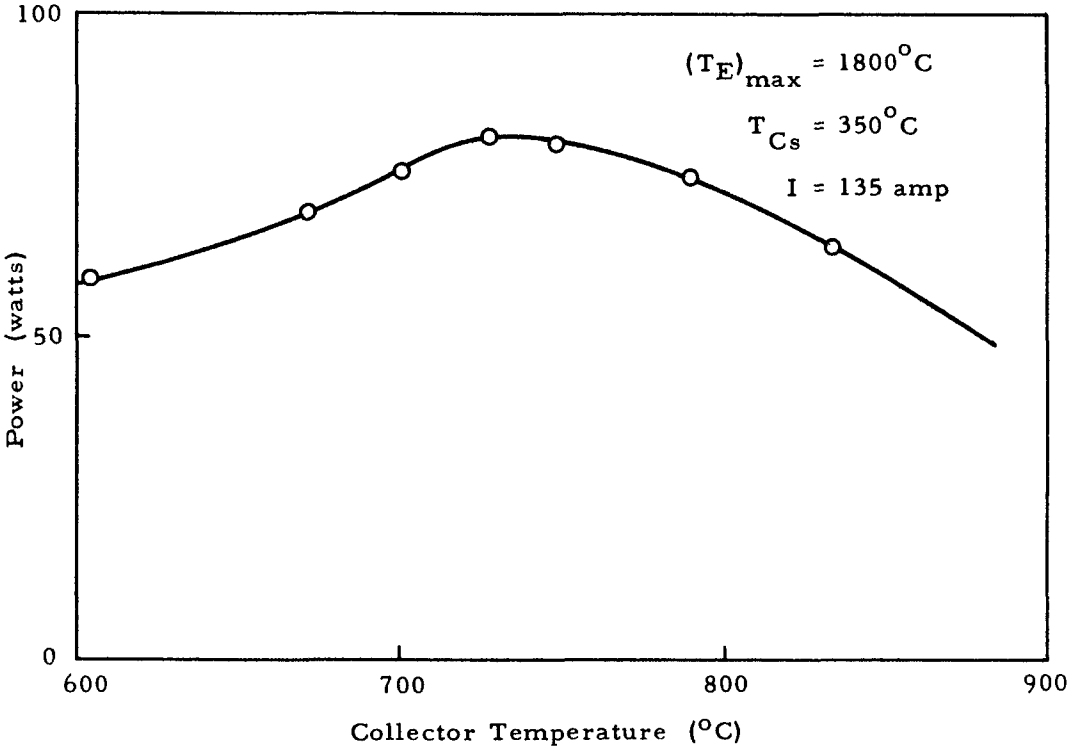

Fig. 3--Initial performance of cell OC-4 (optimization of cesium-reservoir and collector temperatures)

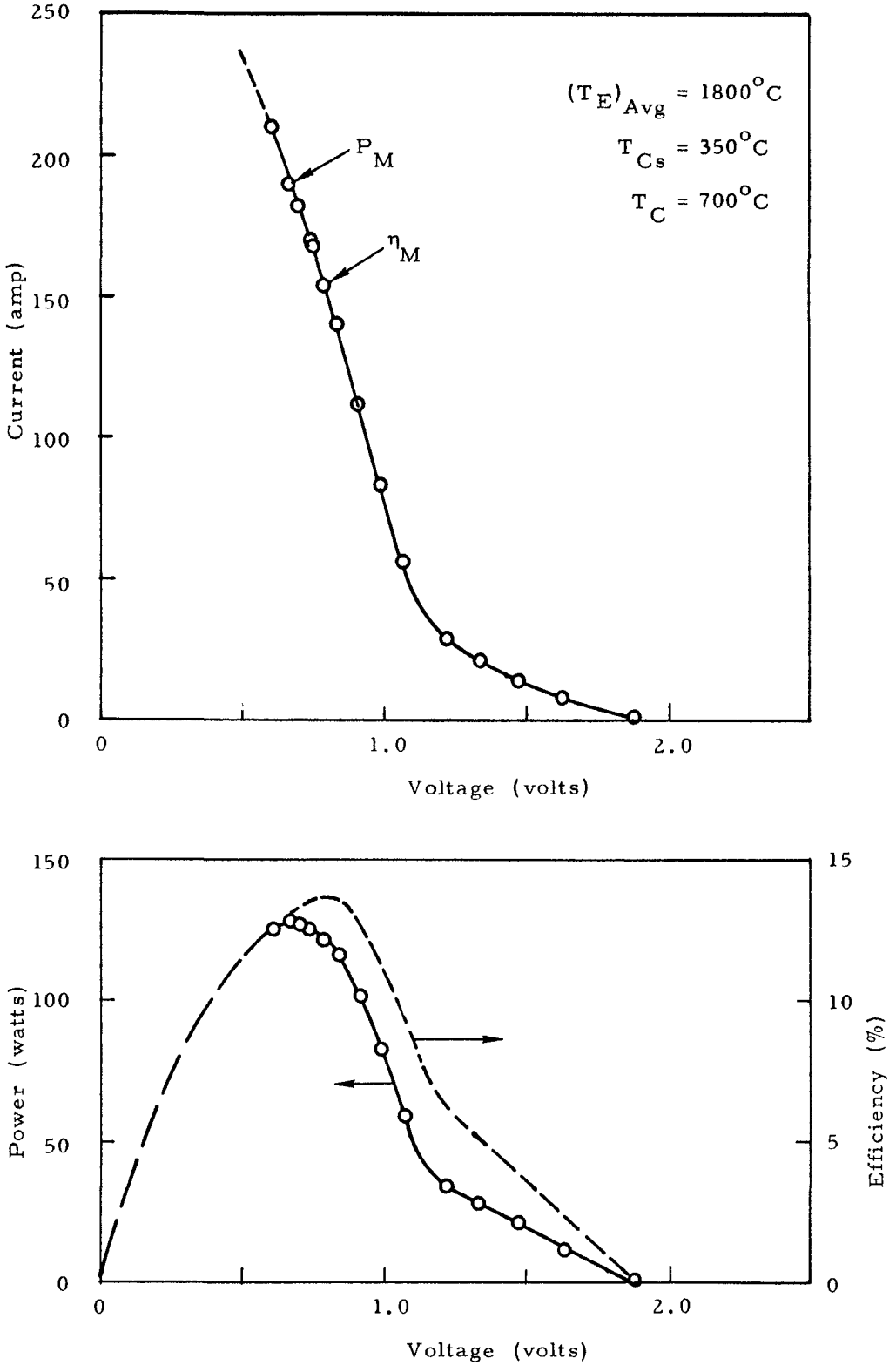

Fig. 4--Initial performance of cell OC-5 (I-V characteristic and optimization of load resistance)

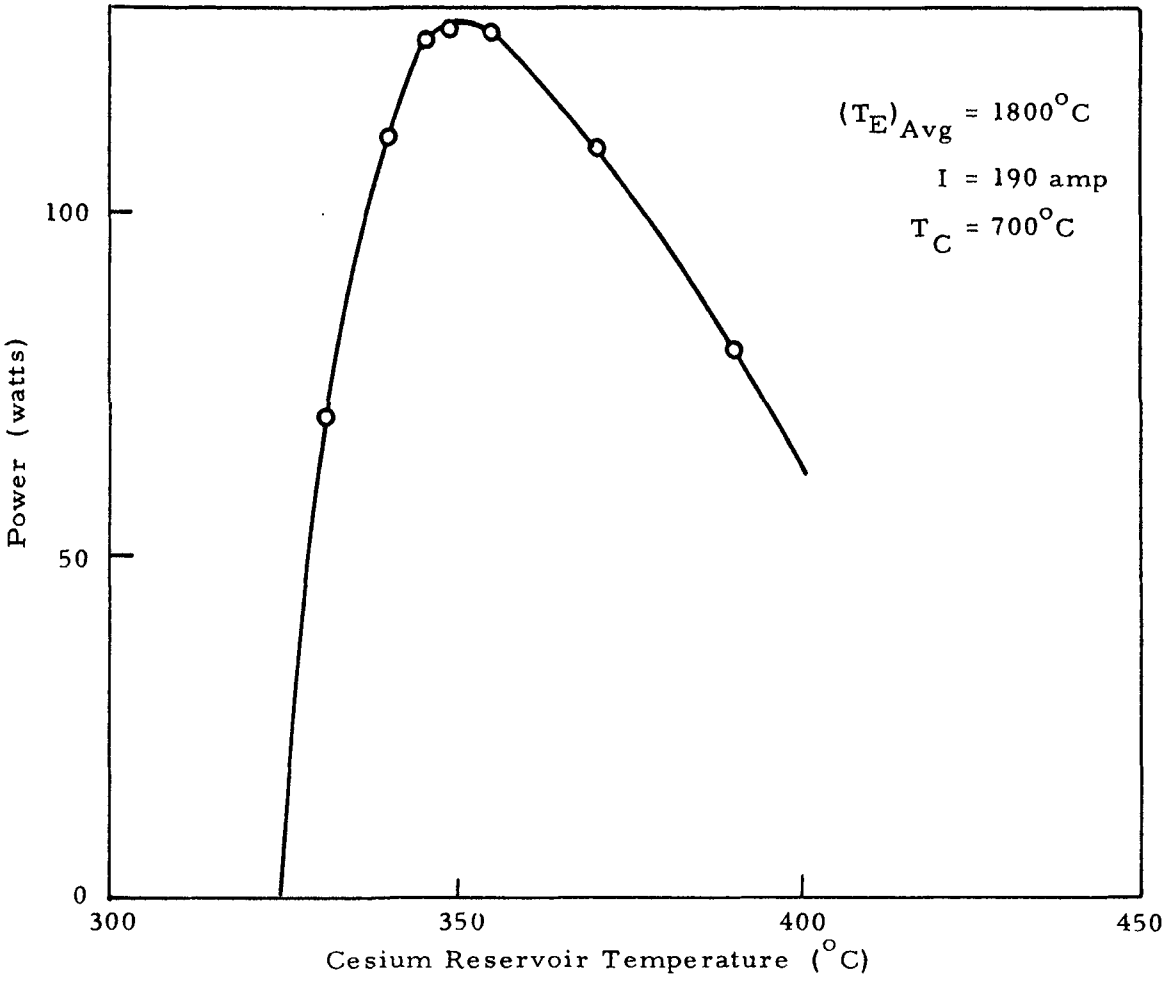

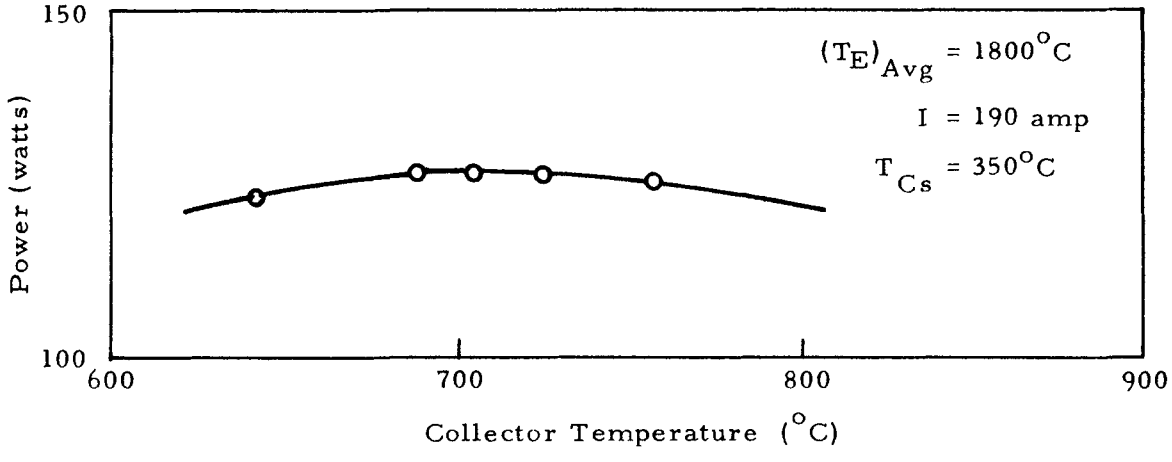

Fig. 5--Initial performance of cell OC-5 (optimization of cesium-reservoir and collector temperatures)

temperature. If OC-5 were compared with OC-4 on the basis of an average emitter temperature of 1750°C, it would have had a power output of 8% less than is reported at 1800°C. Even with this allowance, OC-5 has a power density 60% greater than that of OC-4.

Maximum power measurements for OC-5 were also obtained at emitter temperatures of 1200°, 1400°, and 1600°C. In Fig. 6 the maximum power density and efficiency at the electrodes are plotted as functions of emitter temperature. The resulting curves are nearly linear between 1200° and 1800°C. It is interesting to note that powers of 5 watts/cm^2 are obtained at emitter temperatures as low as 1450°C.

Examples of emitter temperature distributions for these converters are shown in Figs. 7 and 8. These surface temperature distributions are derived from the internal thermocouple temperatures. In Fig. 7 the OC-4 data represent three different experimental conditions:

(1) $I = 0$ and $T_{Cs} = 117^{\circ}C$,
(2) $I = 0$ and $T_{Cs} = 349^{\circ}C$,
(3) $I = 130$ amp and $T_{Cs} = 350^{\circ}C$.

It is seen that the resulting surface temperature profile data are nearly identical for these cases. A slight increase of the temperature near the lead is detectable, however, as a result of resistance heating of the tantalum emitter lead.

Also indicated on the Fig. 7 curve is the average value of the emitter-temperature data and the integrated mean value of the curve--values of 1760° and 1750°C, respectively. It is interesting to note that the mean and the average differ by only 10°C. Because of this close correlation between the predicted mean and the measured average for this temperature level and for the other temperature levels investigated, it is sufficient to report the average and assume that this represents the mean emitter temperature. This is warranted since the measured differences are within the relative errors.

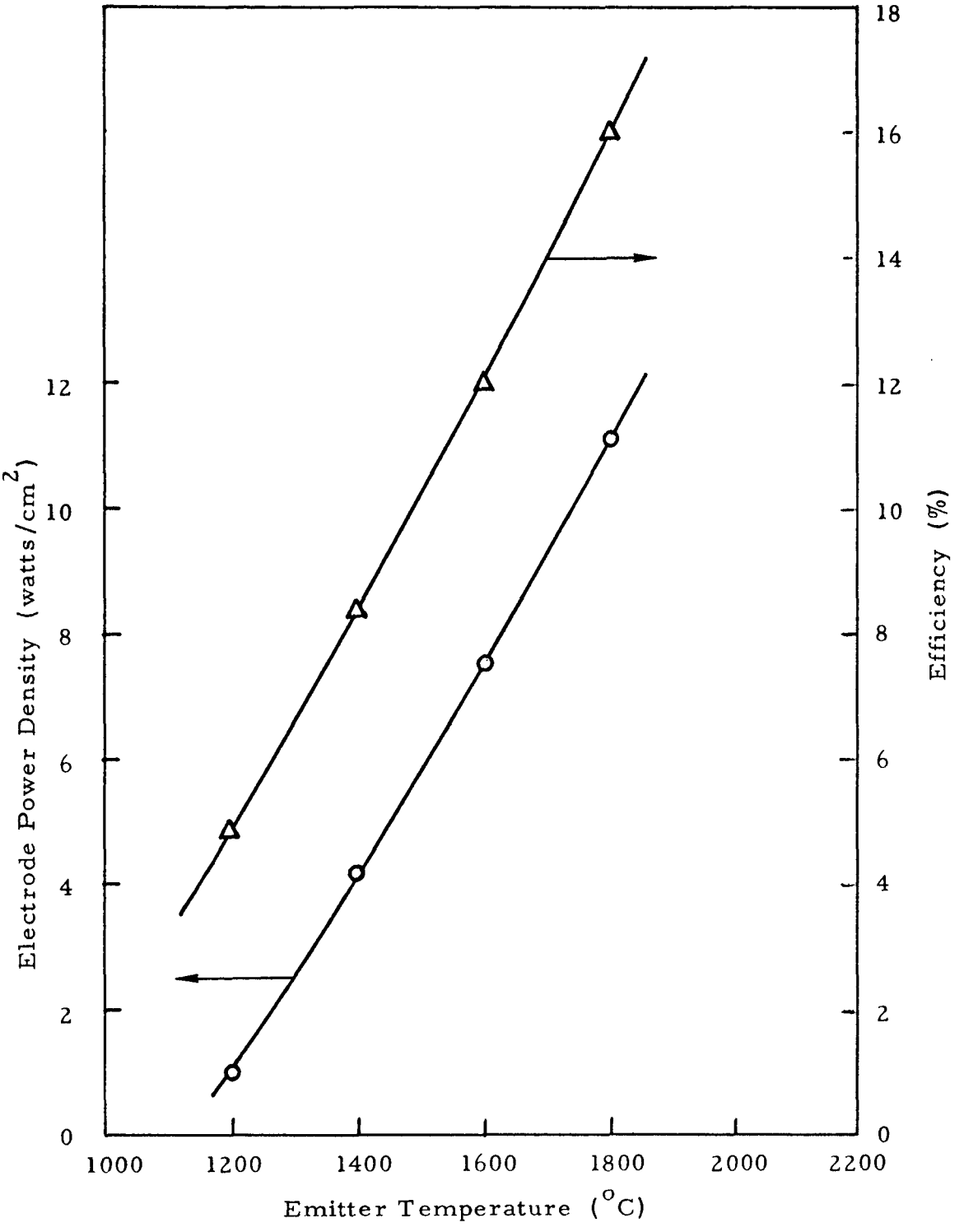

Fig. 6--OC-5 maximum electrode performance at various emitter temperatures

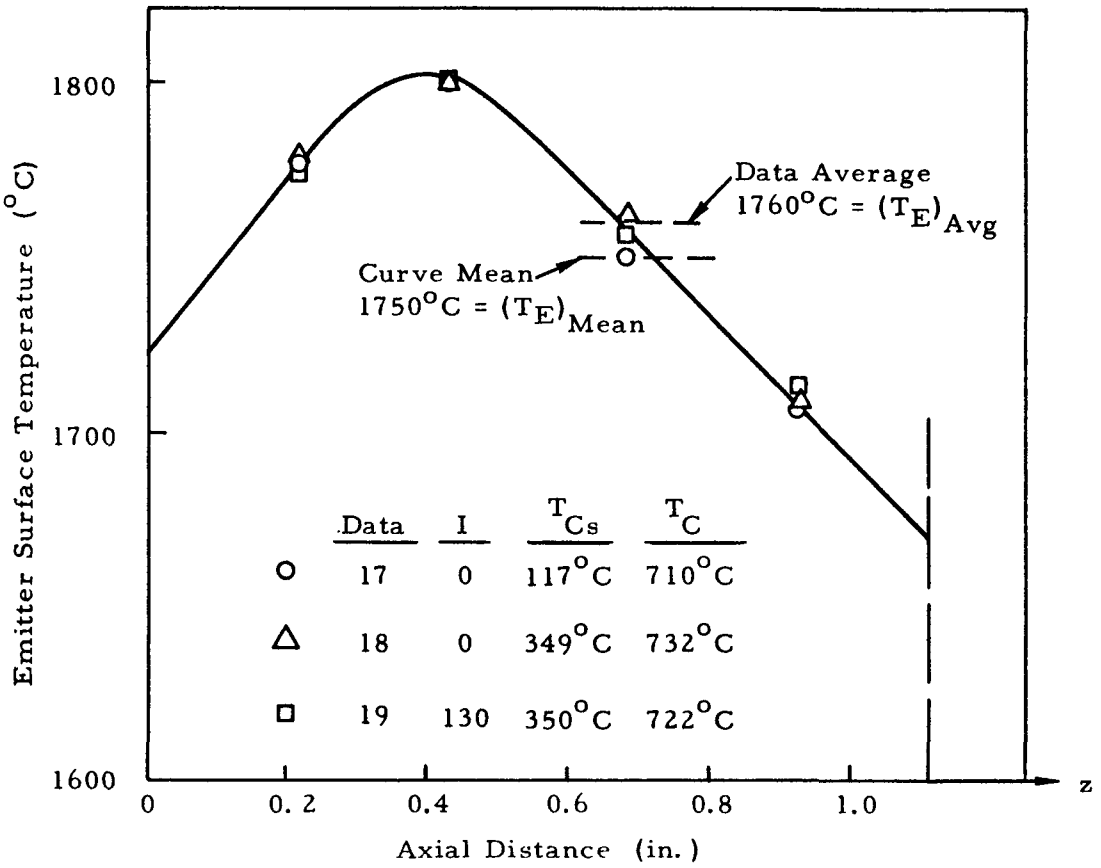

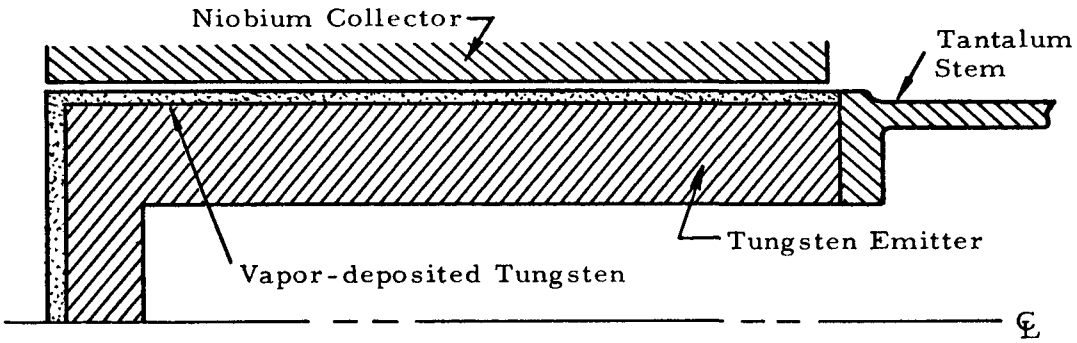

Fig. 7--OC-4 emitter temperature distributions at $(T_E)_{max}$ = 1800°C

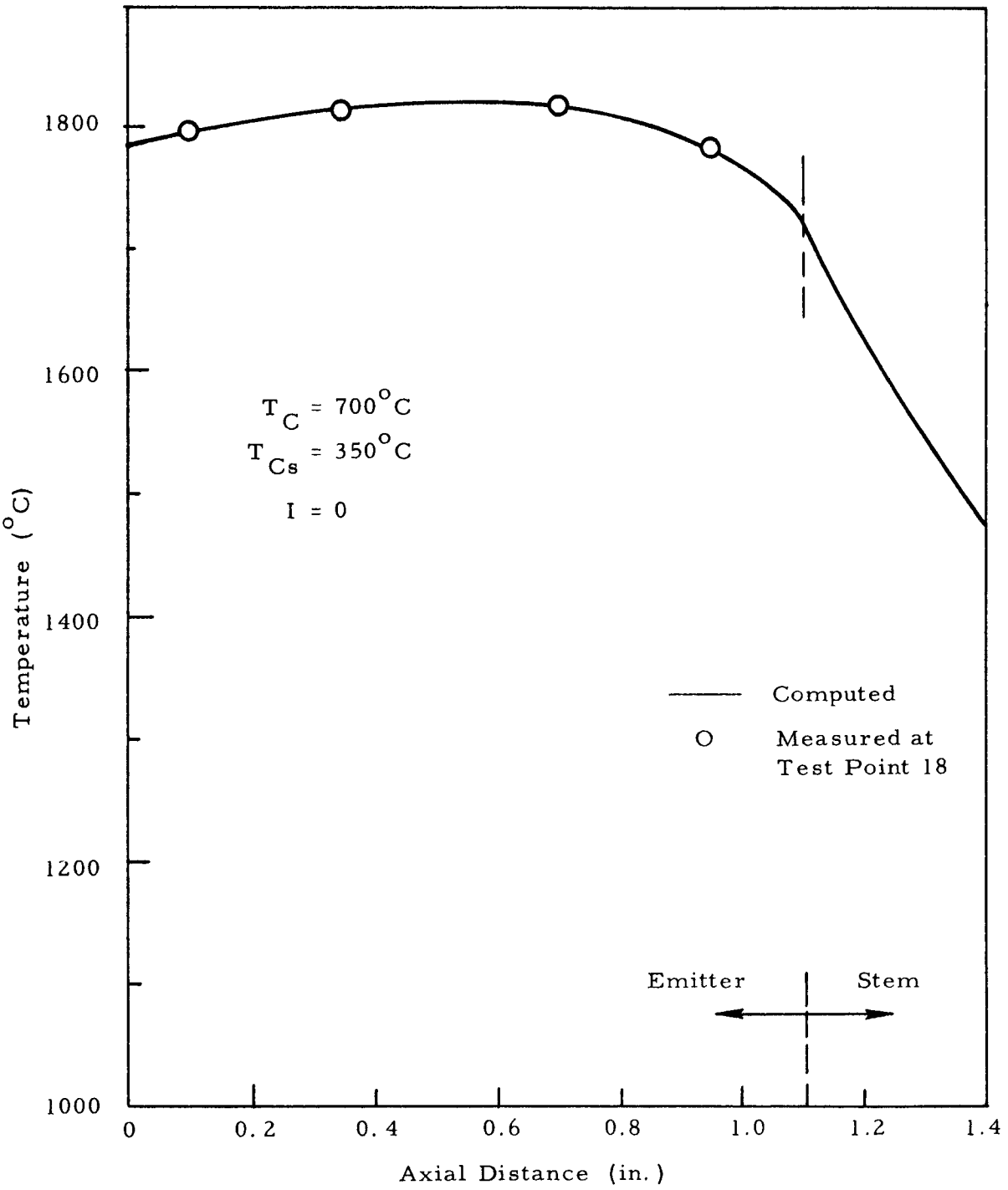

Fig. 8--OC-5 emitter temperature distribution at $(T_E)_{max}$ = 1800°C

The OC-5 emitter temperature-distribution data are shown in Fig. 8 for a single test point. The solid line is the computed emitter temperature distribution, which demonstrates that the values obtained with the digital-computer heat-transfer codes compare well with measurements. The predicted mean emitter temperature and the measured data average agree within $5^{\circ}C$.

Upon comparing the OC-4 and OC-5 temperature distributions, one may note that the latter is more uniform. This result is expected, because of the thicker OC-5 emitter wall.

IV. PERFORMANCE MAPPING

The objective of the mapping is to provide input and output data that are convenient for the analysis of thermionic reactor systems. From the data obtained in the preliminary experiments and from systems-analysis considerations, it was decided that the range of the variables be specified as follows: emitter temperature, 1200° to $1800^{\circ}C$; cesium temperature, 300° to $400^{\circ}C$; collector temperature, 600° to $800^{\circ}C$; and load current, from 0 to 10 amp/cm^2 for OC-4, and 0 to 15 amp/cm^2 for OC-5. A typical performance-mapping result is shown in Fig. 9, where the cell voltage is given as a function of total emitter power with the parameters of current density and emitter temperature. The entire diagram was constructed at a constant cesium temperature of $350^{\circ}C$ and a collector temperature of $730^{\circ}C$.

When the performance results are obtained in this form, thermionic systems containing converters with unequal power inputs may be analyzed conveniently. For example, the total power output from an electrical series of converters may easily be obtained by adding the voltages obtained from a constant-current curve. The result would be for the case where all the converters are operated at one cesium temperature and one collector temperature. Other graphs similar to Fig. 9, but at other cesium and collector temperatures, permit performance calculations of systems where

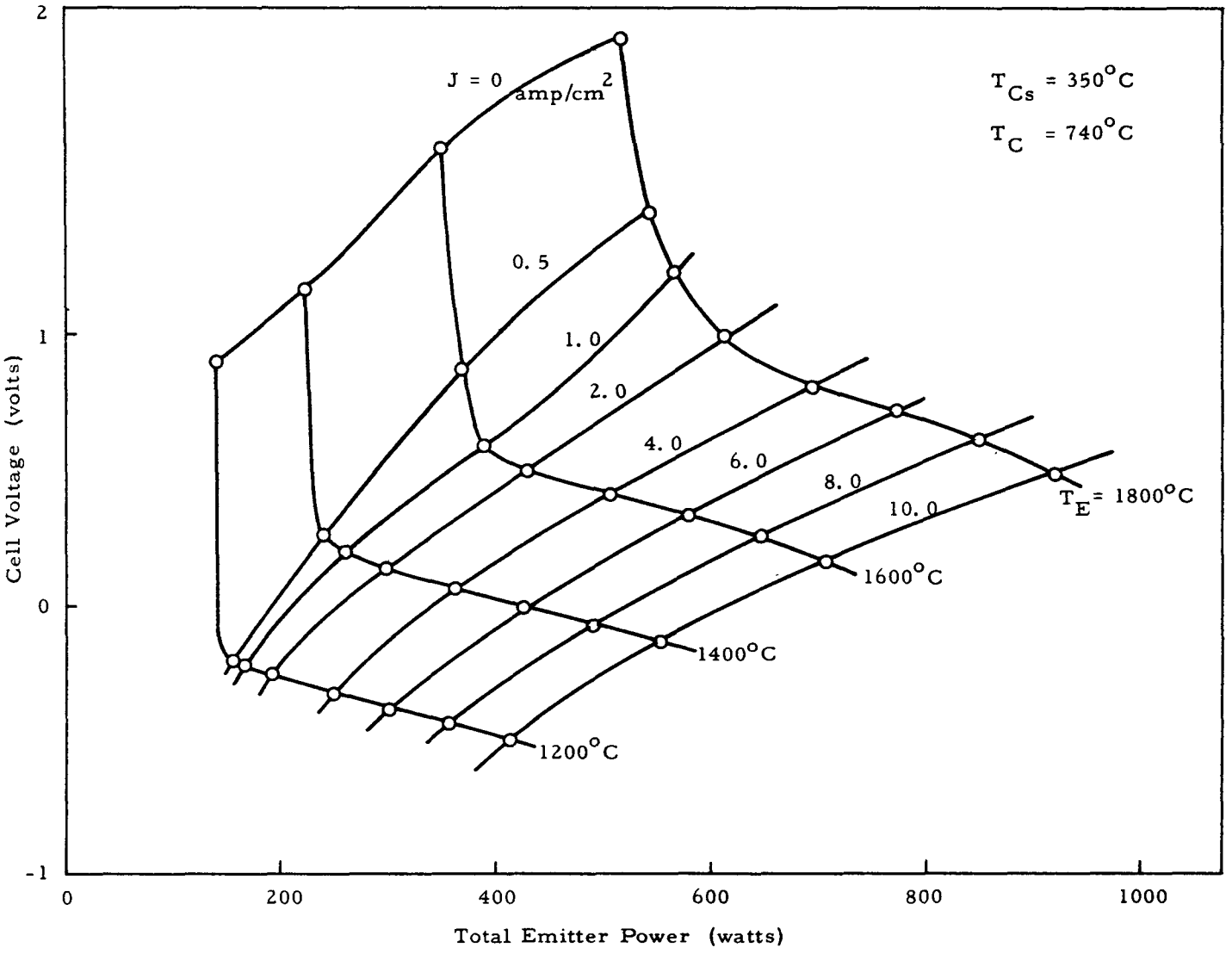

Fig. 9--Performance map of OC-4

the individual converters do not have equal cesium and collector temperatures.

A code has been developed at General Atomic[2] whereby data of this type can be submitted to the library of FORTRAN data in order that automatic interpolation may be performed over the entire range of variables investigated. This offers the analyst a convenient method of calculating systems performance in cases where each converter, whether operated in series or in parallel circuit, can have different operating characteristics.

It should be noted, however, that the results reported herein apply only to cells which have similar geometries and materials. What is actually needed are generalized expressions from which the analyst can compute the power required to operated thermionic converters that have any geometry or materials. A first step towards this goal has been achieved through the energy measurements which are described in the following sections.

V. ENERGY MEASUREMENTS AND ANALYSIS

5.1. Equations for Energy Conservation

Energy-conservation equations for the filament, emitter, collector, and calorimeter are derived from the terms depicted in Fig. 10. The electrical power to the emitter filament chamber Q_F is the sum of a-c resistance heating and electron-bombardment power. Q_F is dissipated by emitter surface heating Q_E; by the various thermal conduction and radiation losses of the emitter structure and filament, Q_{r1}, Q_{k1}, Q_{r4}, Q_{k4}; and by electrical leakages Q_{IL}, as formalized by Eq. (1):

$$Q_F = Q_E + Q_{r1} + Q_{k1} + Q_{r4} + Q_{k4} + Q_{IL} = Q_E + Q_{EL} + Q_{IL} , \qquad (1)$$

where Q_{EL} is the sum of all the emitter structure and filament thermal losses.

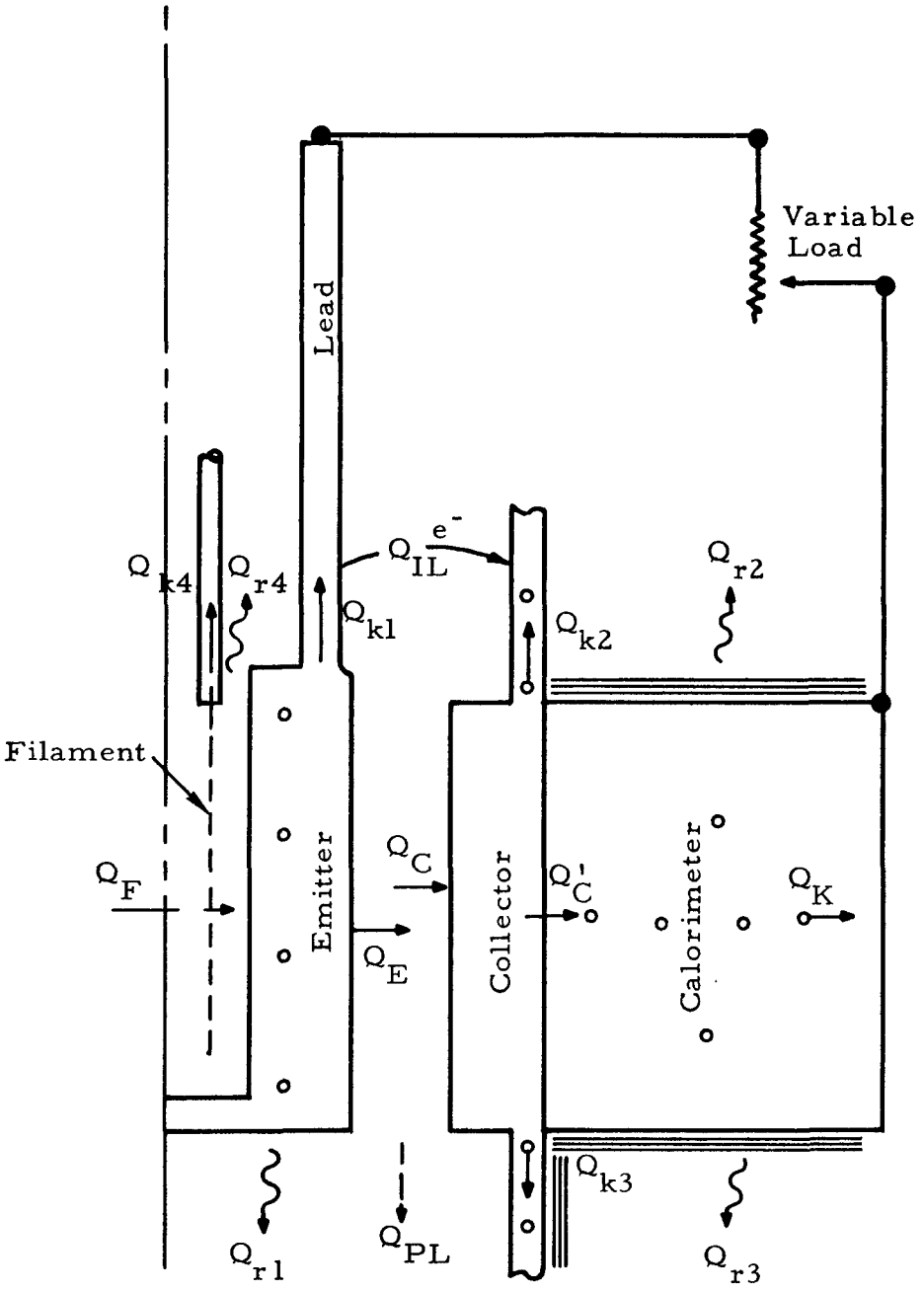

Fig. 10--Terms for energy conservation of converter components

The energy leaving the emitter surface goes to collector heating Q_C to provide electrons with an energy that will be dissipated in the emitter lead and the load IV, and to supply energy leakage from the plasma at the ends of the cylindrical interelectrode space, $Q_{PL} = Q_{p1} + Q_{p2}$, or

$$Q_E = Q_C + IV + Q_{PL} \quad . \tag{2}$$

Equations (3) and (4) account for the heat to the collector surface Q_C and the heat to the calorimeter inner surface Q_C':

$$Q_C = Q_C' + Q_{k2} + Q_{k3} \quad , \tag{3}$$

$$Q_C' = Q_K + Q_{r2} + Q_{r3} \quad . \tag{4}$$

From calorimeter-calibration experiments, it was found that Q_{r2} plus Q_{r3} is much less than Q_K, and can be neglected since their values are well within the experimental errors of determining Q_K. Under this consideration, Q_C reduces to

$$Q_C = Q_K + Q_{k2} + Q_{k3} \quad . \tag{5}$$

For each experimental point, Q_K, Q_{k2}, and Q_{k3} are calculated from measured temperature gradients and literature values of the material thermal conductivity.[3] Q_C is a measured quantity through Eq. (5) and the correlation of Appendix B. Experimental values of Q_F are accurately measured to within about 1%. The power dissipated in the emitter lead and the load IV is also a measured quantity within about 1% acccracy. The remaining unknown values are Q_E, Q_{EL}, Q_{IL}, and Q_{PL}. If Eqs. (1) and (2) are combined,

$$Q_{EL} + Q_{PL} + Q_{IL} = Q_F - (Q_C + IV) \quad . \tag{6}$$

Since all the terms on the right-hand side of Eq. (6) are measured, the sum of Q_{EL}, Q_{IL}, and Q_{PL} is also a measured quantity. With these terms separately unknown, Q_E from Eq. (2) also remains unknown.

The quantities of emitter electron cooling and collector electron heating are derived from subtracting Q_E and Q_C at zero current from values of Q_E and Q_C at non-zero currents:

$$\Delta Q_E = (Q_E)_I - (Q_E)_{I=0} , \tag{7}$$

$$\Delta Q_C = (Q_C)_I - (Q_C)_{I=0} . \tag{8}$$

It is noted that to call the quantities given in Eqs. (7) and (8) electron cooling or heating is actually a misnomer, since ion currents and resonance radiation from the plasma may also contribute to these quantities.[4]

Values of ΔQ_C are directly measured, but ΔQ_E can only be determined by combining Eqs. (2), (7), and (8):

$$\Delta Q_E = \Delta Q_C + IV + \Delta Q_{PL} , \tag{9}$$

where ΔQ_{PL} is defined in a similar manner as in Eqs. (7) and (8). Because the ratio of the plasma end areas to the emitter area is very small, it is assumed that ΔQ_{PL} can be neglected in the following analysis of the experimental data. Hence, under that assumption, ΔQ_E is a measured quantity through Eq. (10) since ΔQ_C and IV are experimentally determined:

$$\Delta Q_E \cong \Delta Q_C + IV . \tag{10}$$

5.2. Energy-loss Measurements and Calculations at Zero Currents

The total power input to the emitter filament chamber is either dissipated as thermal loss or is converted into electrical power delivered to the load. At zero-current operation, therefore, all of the power input is dissipated as energy loss. The energy quantities measured at zero current are the total power input to the filament chamber Q_F, the power intercepted by the collector Q_C, and the cesium thermal conduction from the emitter to the collector. In Table 3 the data for a single test point are shown, along with computed loss values. Heat losses from other than the emitting surface are Q_F minus Q_C, which for this case is 200 watts.

Table 3

MEASURED AND CALCULATED LOSS VALUES
FOR TEST POINT 18, CONVERTER OC-5

Measured Data

Q_F	469 watts
Q_C	269 watts
I	Zero
T_E	1800°C
T_C	700°C
T_{Cs}	350°C
$Q_{EL} = Q_F - Q_C$	200 watts

$Q_{EL} = Q_{rl} + Q_{kl} + Q_{r4} + Q_{k4}$

Computer Results

Q_{rl}	47 watts
Q_{kl}	102 watts
$Q_{r4} + Q_{k4}$	~40 watts
$(Q_{EL})_{Calc}$	189 watts
Cesium thermal conduction (determined experimentally)	51 watts
Heat transferred by radiation	269 - 51 = 218 watts
Electrode effective emissivity	0.157
Emitter emissivity (from previous experiment)	0.349
Collector emissivity	0.222

These emitter structural losses are the sum of the thermal radiation from the emitter end, the thermal conduction in the emitter lead, the thermal radiation from the filament chamber, and the thermal conduction from the filament leads. This total value was calculated with an IBM-7090 digital computer to be 189 watts, which is a close comparison to the 200-watt loss experimentally determined.

Cesium thermal conduction between the converter electrodes was previously determined experimentally at 51 watts, which compares closely to values predicted by Kitrilakis amd Meeker.[5] The heat transferred by radiation between the electrodes is 218 watts, which is the difference between the collector heat and the cesium thermal conduction. From the radiation heat, the interelectrode effective emissivity is calculated to be 0.157. The emitter total emissivity is known from previous experiments to be equal to 0.349 at an emitter temperature of 1800°C. There results a collector emissivity of 0.222. It may be noted at this point that it is possible to predict analytically all of the energy-transfer quantities observed for a zero-current case.

5.3. Energy Measurements at Non-Zero Currents

Energy measurements were made over the same range of operating variables that the performance-mapping experiments covered. This range included: emitter temperature of 1200° to 1800°C, cesium reservoir temperature of 300° to 400°C, collector temperature of 600° to 700°C, and current of zero to 15 amp/cm^2 (where possible). A few typical examples of the energy measurements are shown in Figs. 11 and 12, where the values of Q_F, Q_C, IV, and $(Q_C + IV)$ are shown as a function of converter current density. Both of these examples are at an emitter temperature of 1800°C and a collector temperature of 700°C. The difference between the operating conditions of Fig. 11 and Fig. 12 is the cesium reservoir temperature. The "collector electron heating" and "emitter electron cooling" energies are determinable from these data and from Eqs. (7) and (8).

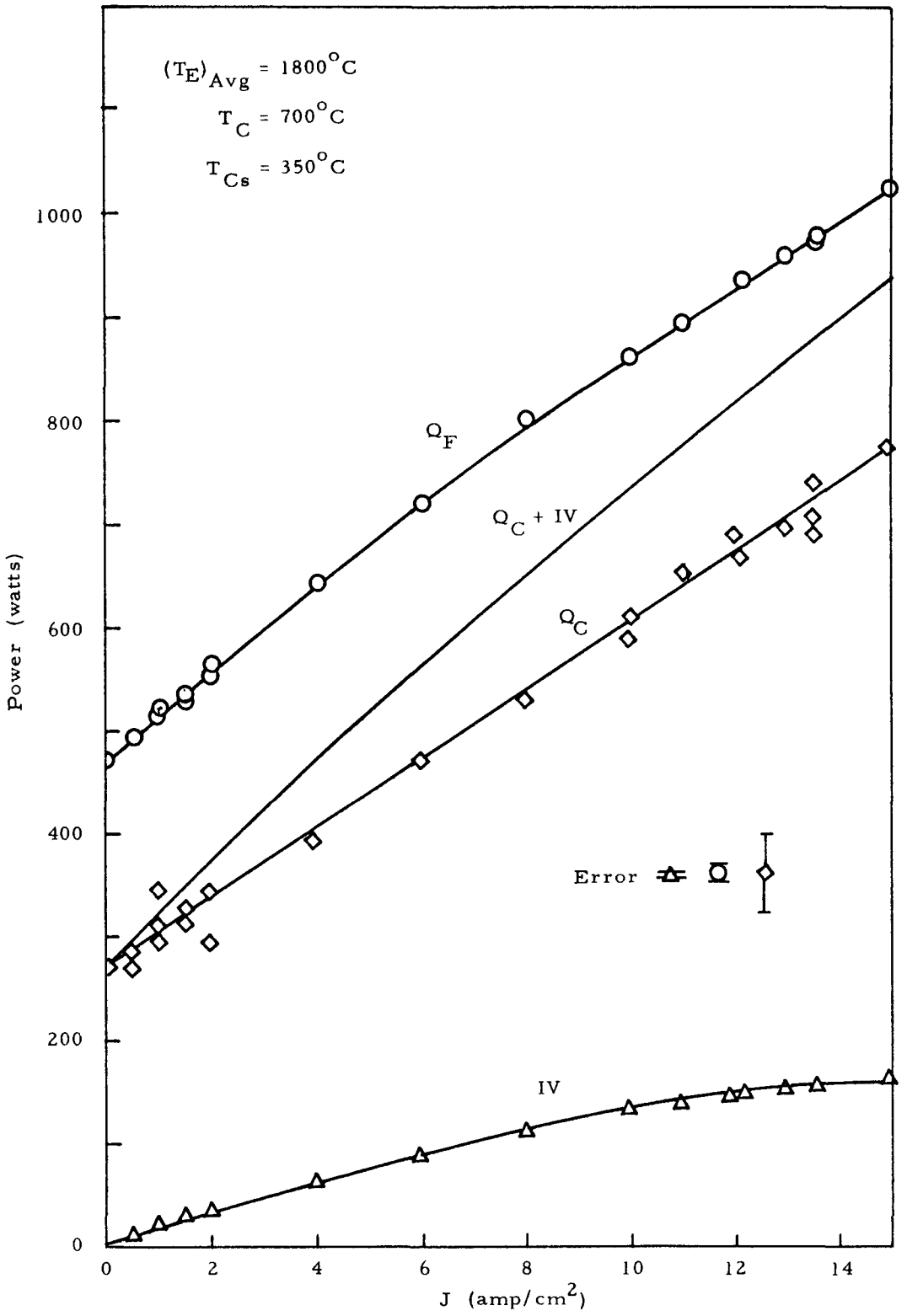

Fig. 11--OC-5 energy measurements at T_{Cs} = 350°C

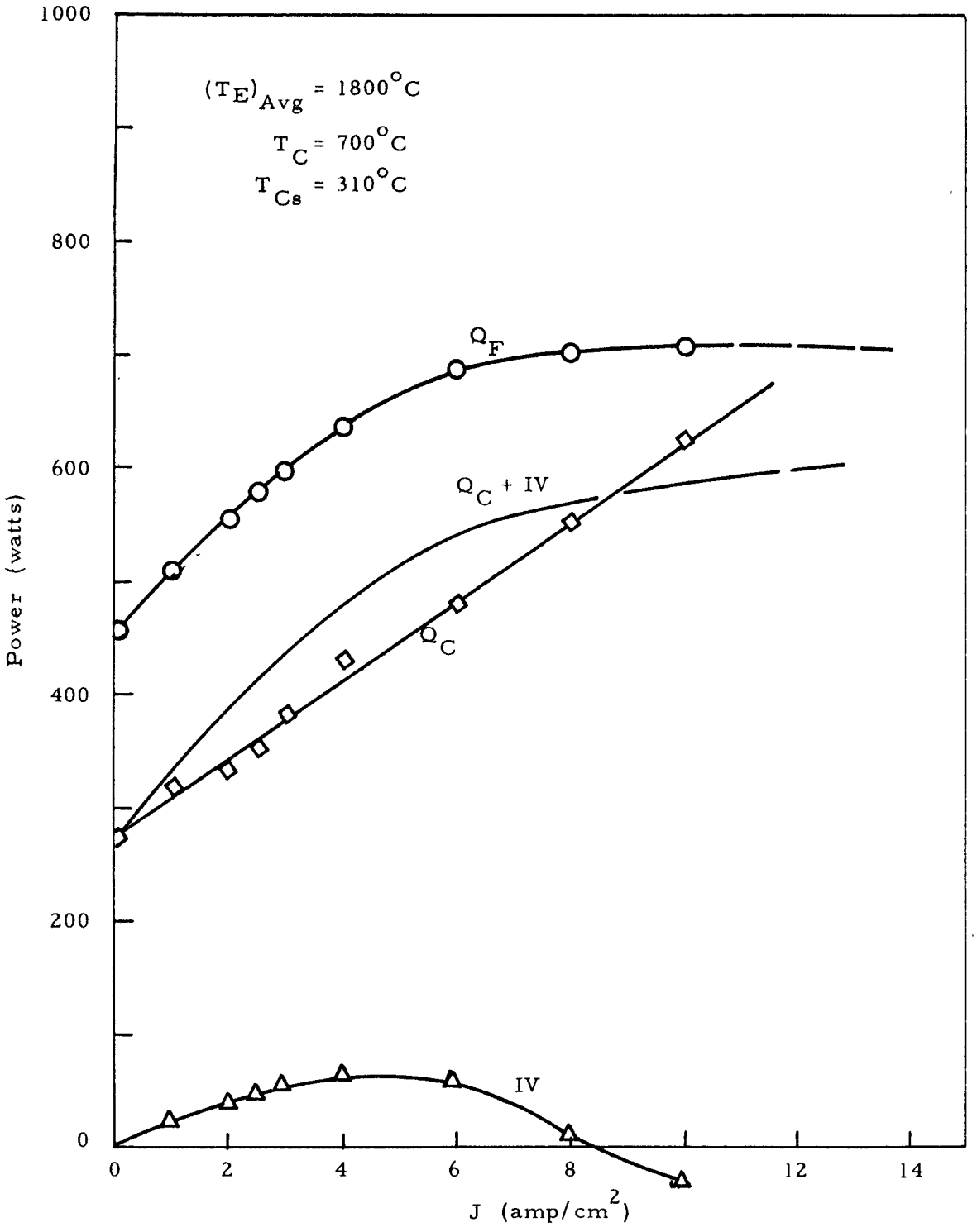

Fig. 12--OC-5 energy measurements at T_{Cs} = 310°C

In Figs. 11 and 12 the Q_F curves are found to be not parallel with the $(Q_C + IV)$ curves. The implication of this result is that the sum of ΔQ_{IL}, ΔQ_{PL}, and ΔQ_{EL} is a negative quantity, as would be derived from Eq. (7). It is probable that ΔQ_{EL} is a negative quantity due to the fact that heat is conducted back to the emitter from resistance heating in the emitter lead. The maximum value this could have, however, would be 15 watts when J is 14 amp/cm^2, since the total measured power generated in the stem due to resistance heating is 30 watts. The remainder of the difference, then, must be due to changes in emitter temperature distribution, in emitter voltage distribution, in Q_{PL}, or in Q_{IL}. No definite conclusions regarding these differences can be made, however, since the envelope of the calorimeter errors nearly encompasses the remaining differences. A further improvement in the precision of calorimetric measurements would be of value in understanding these differences.

VI. EMITTER ELECTRON-COOLING CORRELATION

It is interesting to note that the Q_C curves in Figs. 11 and 12 are linear functions of J and have nearly equal slopes. Furthermore, for all the cases studied it is found that Q_C versus J curves have derivatives of 2.6 ±0.2 watts/amp. The range of variables covered in the experiment included emitter temperature of 1200° to 1800°C, cesium temperature of 300° to 400°C, and collector temperature of 600° to 700°C.

With the value of dQ_C/dI known to within the errors indicated, it is clear that one may determine with fair accuracy the energy quantities due to emitter electron cooling by substituting the value of ΔQ_C into Eq. (10), obtaining the result:

$$\Delta Q_E = \Delta Q_C + IV = \frac{dQ_C}{dI} I + IV = I(2.6 + V) . \qquad (11)$$

Emitter electron cooling is therefore predicted from Eq. (11) if performance characteristics in the form of I-V curves are available. It is noted that the uncertainty of ±0.2 volt in the slope of Q_C represents only an 8% error in determining the collector electron heating. Since the electron cooling

of the emitter usually comprises only one-half or less of the total power input to the emitter, the maximum error using this correlation must be less than 4%. Under most circumstances, the error would be considerably less.

VII. CONCLUSIONS

The electron-cooling correlation, together with the ability to calculate all of the power-loss values in a thermionic converter, makes it possible to compute the efficiency of a converter when the I-V characteristics and materials properties are known. This is an extremely important analytical tool for the analyst to use in computing the performance of complicated systems of thermionic converters where wide variations in the operating variables may occur.

Converter OC-5 with the molybdenum collector gave electrode power outputs of 11 watts/cm^2, which is 60% greater than the output of OC-4 with a niobium collector. This performance difference is greater than would be predicted based only on work-function and thermal-expansion differences. It is postulated that the lower performance of OC-4 was caused by combination effects of larger emitter temperature profile variations and stable resistive layers of niobium oxides that accumulated on the collector surface during fabrication and operation.

REFERENCES

1. Rump, B. S., private communication, October 28, 1963.
2. Broido, J., C. Savery, and W. Wright, A Digital Computer Code for the Analysis of Thermionic Networks, General Atomic Report GA-4147, May 22, 1963.
3. Goldsmith, A., T. Waterman, H. Hirschhorn, Handbook of Thermophysical Properties of Solid Materials, Rev. Ed., Vol. I: Elements, Macmillan Company, 1961, p. 467.
4. Houston, J., "Measurement of Emitter Heat Balance in a Cesium Thermionic Converter," Twenty-Third Annual Conference, Physical Electronics, March 20–22, 1963, Massachusetts Institute of Technology, 1963, pp. 376–392.
5. Kitrilakis, S., and M. Meeker, "Experimental Determination of the Heat Conduction of Cesium Gas," Advanced Energy Conversion, Vol. 3, January–March, 1963, pp. 59–68.

Appendix A

EMITTER SURFACE TEMPERATURE DISTRIBUTION EXPERIMENT

In this experiment, correlations were developed for determining emitter surface temperatures from internal thermocouple readings. This is done with a test emitter outside a cell by measuring temperature differences between internal thermocouples and optical hohlraums in the emitter surface. The brightness temperatures of the emitter are measured at the same time, so that emissivity correction is obtained for predicting true temperatures on similar surfaces where optical hohlraums are absent.

Concurrently with the experiment, the surface temperature distributions were calculated using a two-dimensional heat-transfer digital computer code (RAT). For a given power input to both the experiment and the computation, the temperature distribution determined in the code results was duplicated by adjusting the thermal emissivities of both the emitter and its lead. Duplication of the temperature distributions and of determination of the emissivities is particularly worthwhile for further correlation work in different geometries, dimensions, or operating conditions. Of special interest is the application to thermionic reactor calculations and in-pile experiments.

The experiment is divided into two parts. First, a test emitter is prepared with optical hohlraums that are used for determining accurate measurements of the true surface temperature distribution. In this first experiment, information is obtained on how to formulate the correlation which will be used at a later time in second and third experiments when the OC-4 and OC-5 emitter surface temperature distributions are correlated to the internal thermocouple temperatures.

APPARATUS

To reduce both the relative and absolute errors in the experiment, calibration measurements were conducted on all of the temperature-measuring instruments and optical windows. Surface-temperature measurements were made with a micro-optical pyrometer which was calibrated against an NBS tungsten ribbon standard. The thermocouples were W/W-26 Re with 1/16-in. -diameter tantalum sheaths. These thermocouples were optically calibrated to within a relative error of $\pm 5^{\circ}$C.

The vapor-deposited tungsten test emitter used in the initial correlation experiment had drilled into its surface five 10-mil-diameter by 70-mil-deep cavities at equidistant axial locations starting and ending 50 mils from the emitter ends. The emitter was heated in a VacIon high-vacuum station at vacuums of 10^{-7} torr. An electron bombardment filament was accurately positioned in the emitter central cavity. The four W/W-26 Re thermocouple junctions were located at four axial positions in holes located within the emitter walls, as illustrated in Fig. A-1. These thermocouples lie 90° apart in the circumferential direction. Two bare W/W-26 Re thermocouples and two Chromel-Alumel thermocouples were spot-welded to the emitter lead for determining the emitter-lead temperature distributions.

EXPERIMENTAL RESULTS

Temperatures of the hohlraums, the emitter surface, the emitter thermocouples, and the emitter lead were determined for varying emitter temperature levels between 1200° and 1800°C. Corrections to the values of the hohlraum temperatures were necessary in order to obtain true emitter surface temperatures, since the temperature measured in the hohlraum is actually hotter by as much as 20°C than the surface temperature. The values of these corrections were determined with the two-dimensional RAT heat-transfer code. Figure A-2 shows the variations of the true surface temperature, the brightness temperature, and the thermocouple

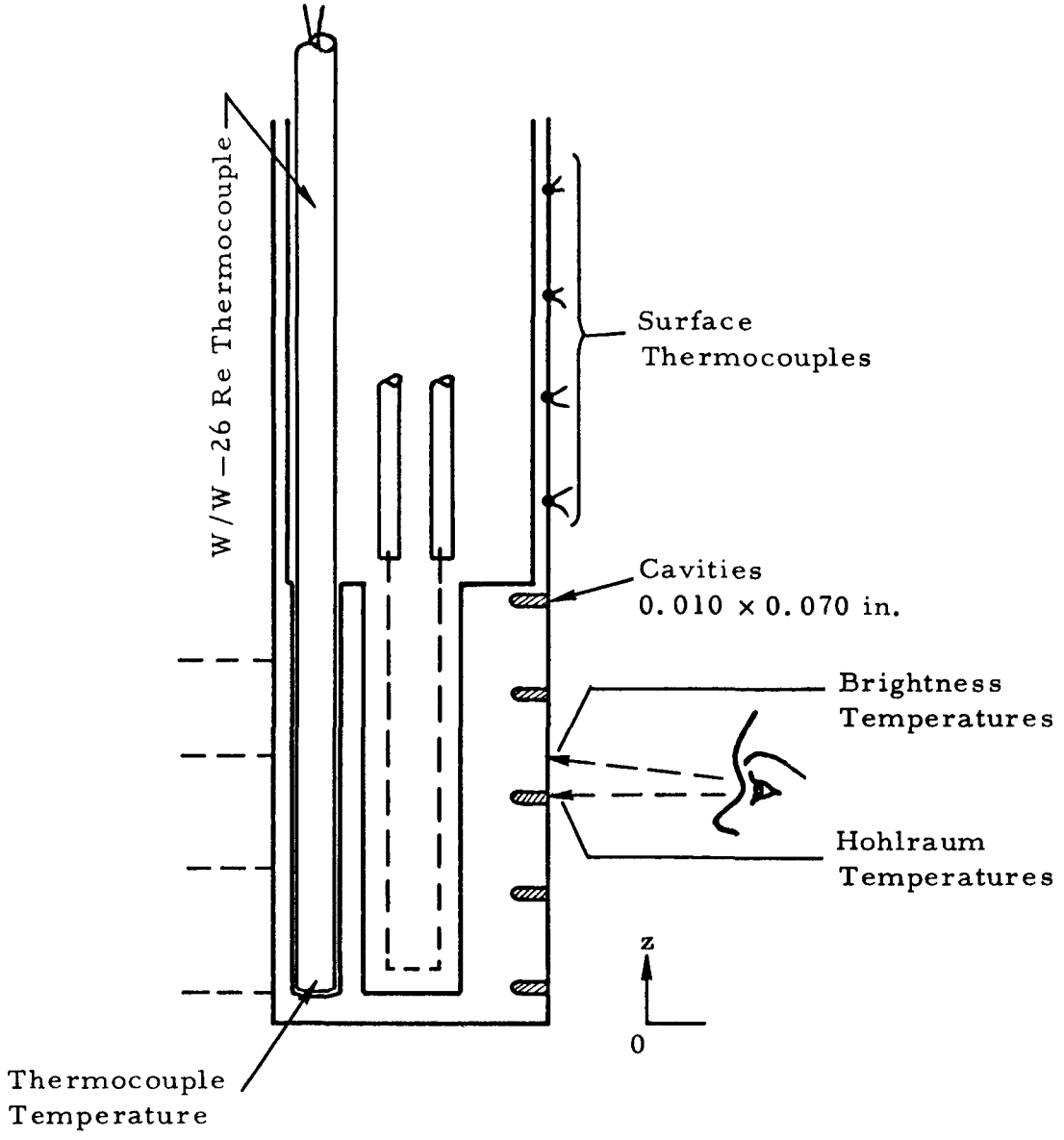

Fig. A-1--Locations of measurements for thermocouple–surface temperature correlation of test emitter

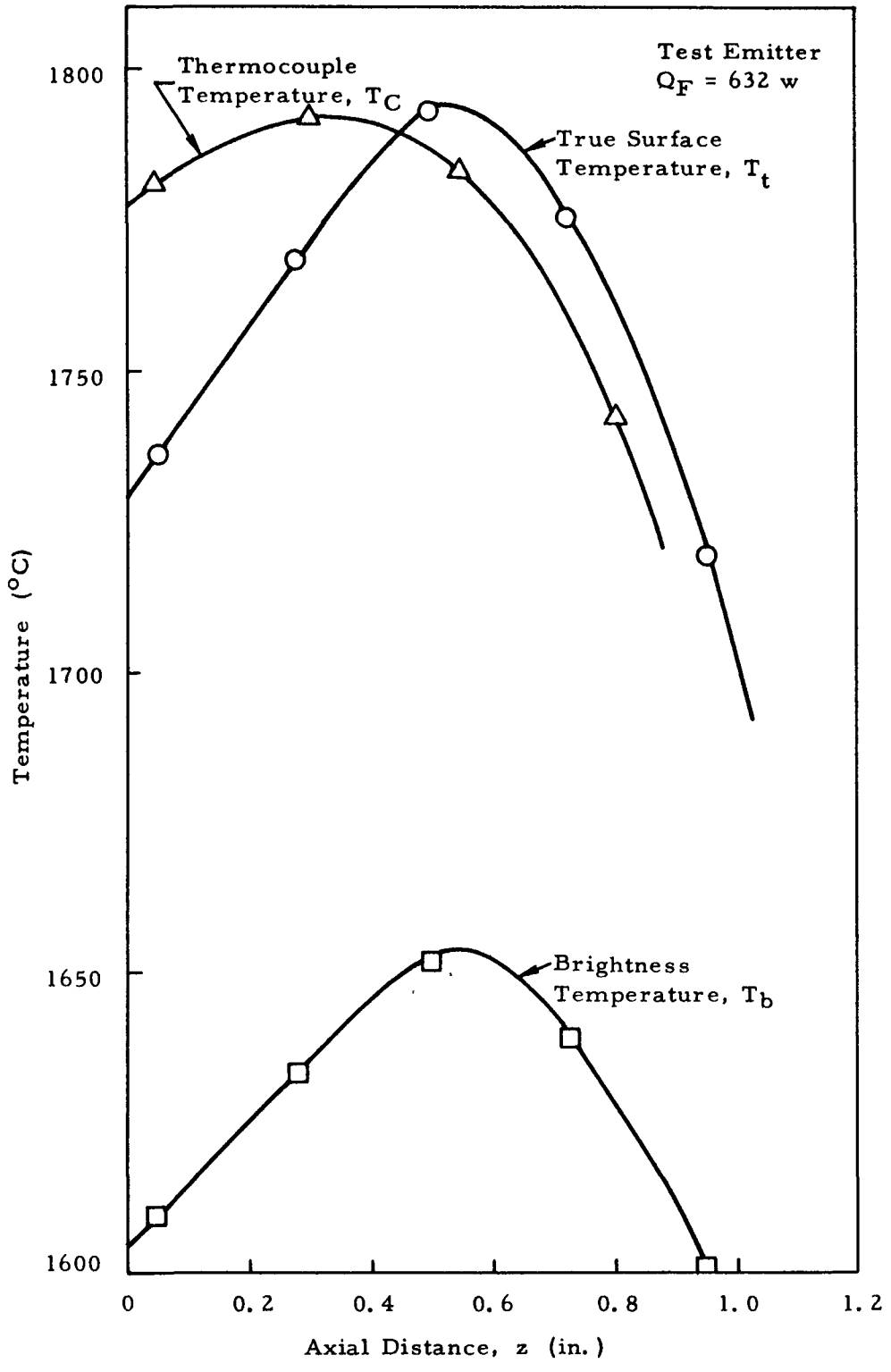

Fig. A-2--Thermocouple–surface temperature correlation of test emitter

temperatures, as a function of the axial surface position z. This is just one example of the temperature levels studied. The difference between the thermocouple and the true surface temperature levels at a given emitter surface position is the correlation required to correct internal thermocouple readings to a true surface temperature.

Upon examining the curves of the brightness temperature and the true surface temperature in Fig. A-2, one finds that the temperature difference between the curves is smaller in the lower-temperature regions. This result is expected, since the brightness correction is actually an increasing function of the true surface temperature.* Figure A-3 shows the brightness correction for the vapor-deposited tungsten emitter as a function of the brightness temperature for the various data obtained. This experimental determination of the brightness correction is important when true temperatures of other emitter surfaces which may not be penetrated with hohlraums are required. Also shown in Fig. A-3 is a curve for a tungsten ribbon filament lamp.*

To establish the emitter surface-to-thermocouple temperature correlation as a function of z and also as a function of the emitter temperature, the same experiment was performed at other temperature levels. In Fig. A-4 an example is shown where three different temperature levels are investigated, with the true surface temperatures and the thermocouple temperatures indicated. The curves are those computed using the RAT heat-transfer code. It was possible to obtain this close correlation of the RAT results with the experimental results by adjusting the total emissivities of the tungsten emitter and the tantalum stem.

The surface-to-thermocouple temperature correlation derived for the test emitter is shown in Fig. A-5 as a function of the maximum emitter temperature and the axial distance from the emitter bottom. These results show that the thermocouple temperature is as much as 40°C greater than

*de Vos, J. C., The Emissivity of Tungsten Ribbon, Thesis, Amsterdam, 1953.

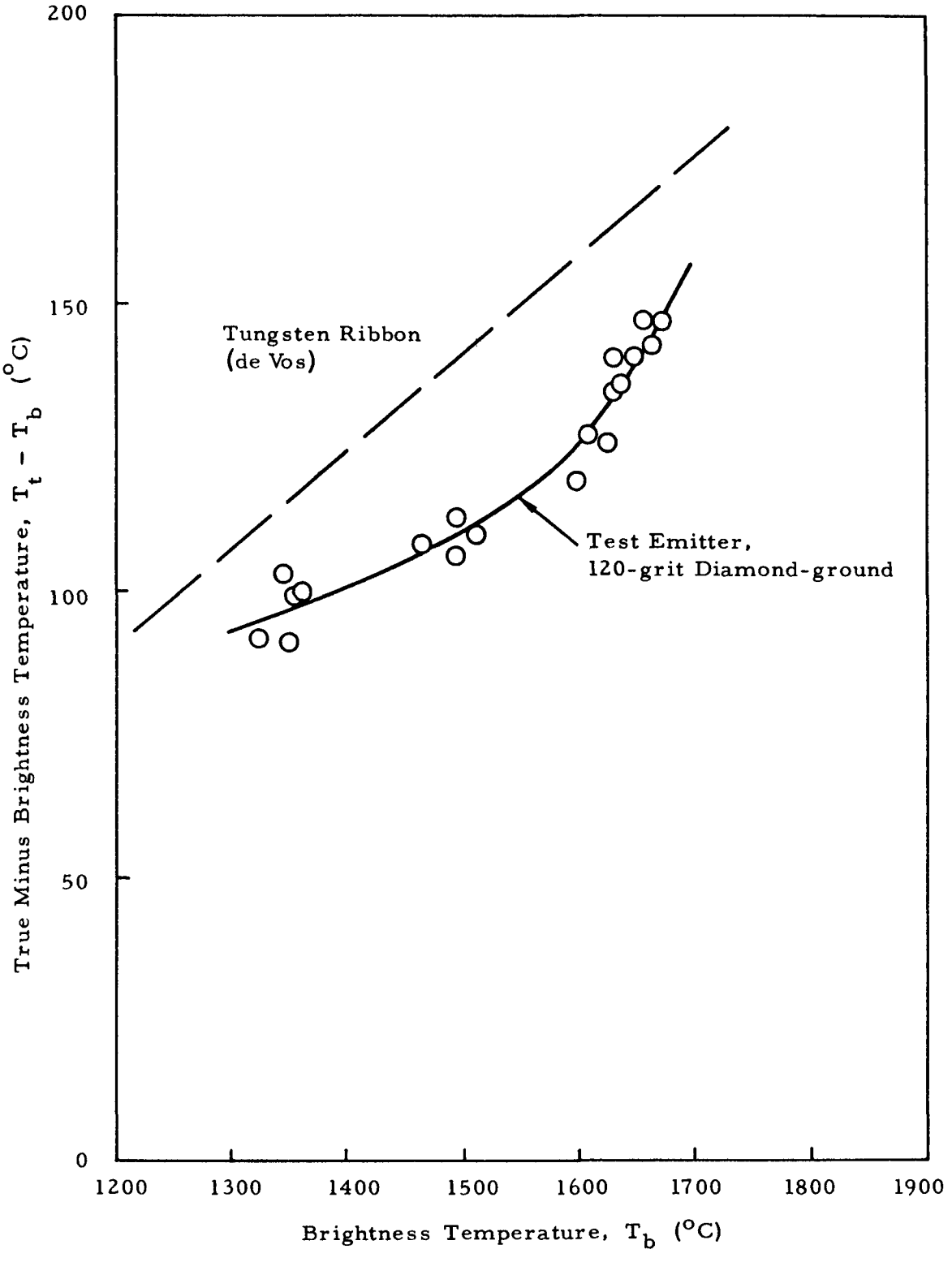

Fig. A-3--Brightness corrections for ground, vapor-deposited tungsten test emitter

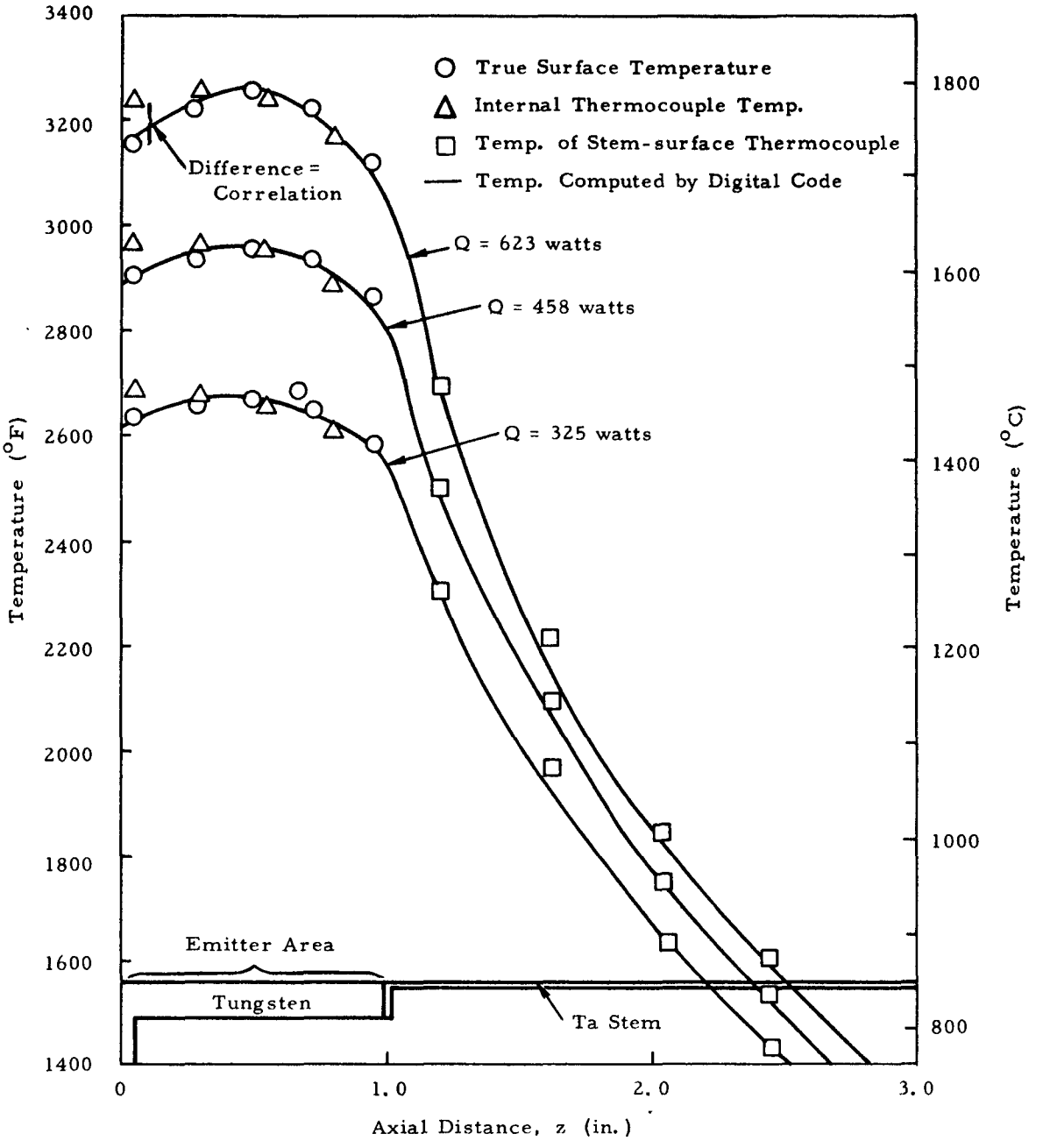

Fig. A-4--Thermocouple—surface temperature correlation of test emitter

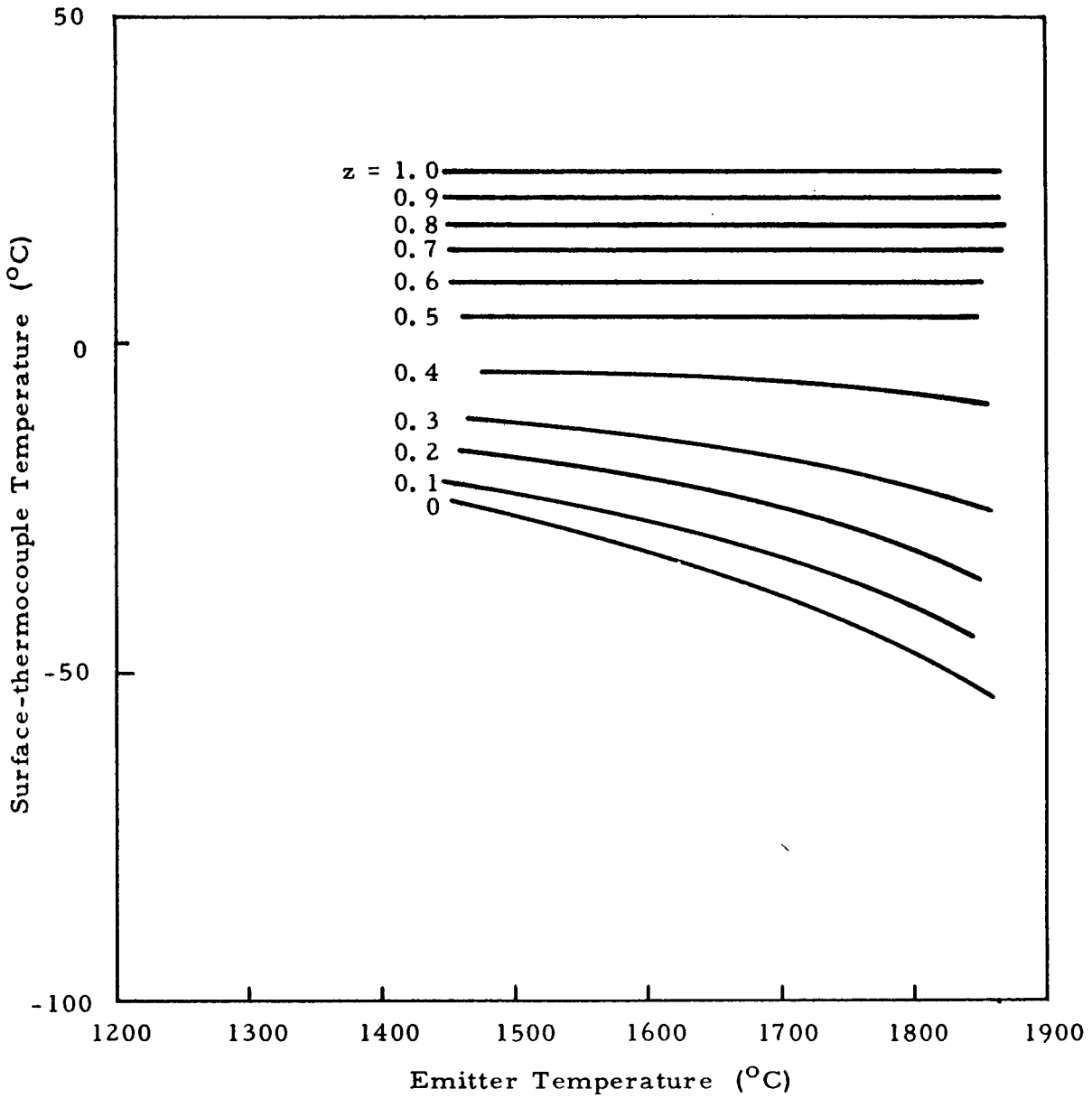

Fig. A-5--Test-emitter correlation of thermocouple and surface temperatures

the surface temperature at low z values. At high z values, the surface temperature reads as much as 10°C greater than that of the thermocouples.

The explanation for this is simply that the thermocouple is heated almost entirely by radiation, with the result that any deviations of the thermocouple from the emitter temperatures are the result of heat conduction through the thermocouple itself. The reason that the thermocouple junction can be hotter than the emitter in low z areas is that the thermocouple sheath is heated to higher temperatures where it passes through the central emitter area. The heat conducts down the sheath and insulation to the thermocouple junction, resulting in higher indicated temperatures than those of the surroundings of the junction.

To determine a surface-to-thermocouple temperature correlation in the emitters to be used in the out-of-pile cells, where hohlraums are not permitted in the emitter surface, only brightness temperatures and thermocouple temperatures may be obtained. The brightness temperatures must then be corrected by the brightness correction given in Fig. A-3, in order to determine true surface temperatures. This was done for the emitters in OC-4 and OC-5; the results are shown in Figs. A-6 and A-7. It will be noted that the correlation results for these emitters are very similar to those obtained for the test emitter. One should not expect an exact comparison between the three cases because the converter-emitter geometry is considerably different from that of the test emitter. Also shown in Figs. A-6 and A-7 are dashed lines representing z-positions of the four thermocouples used in the actual converter test. The values that these curves portray are used to correct the respective thermocouples to true surface temperatures.

Calculations were performed with the heat-transfer code to determine if the additional heat-transfer term of electron cooling greatly affects the emitter temperature profile. It was found that this is a small effect and that the greatest factors influencing the profile are the end losses of thermal conduction in the emitter lead and radiation from the emitter end.

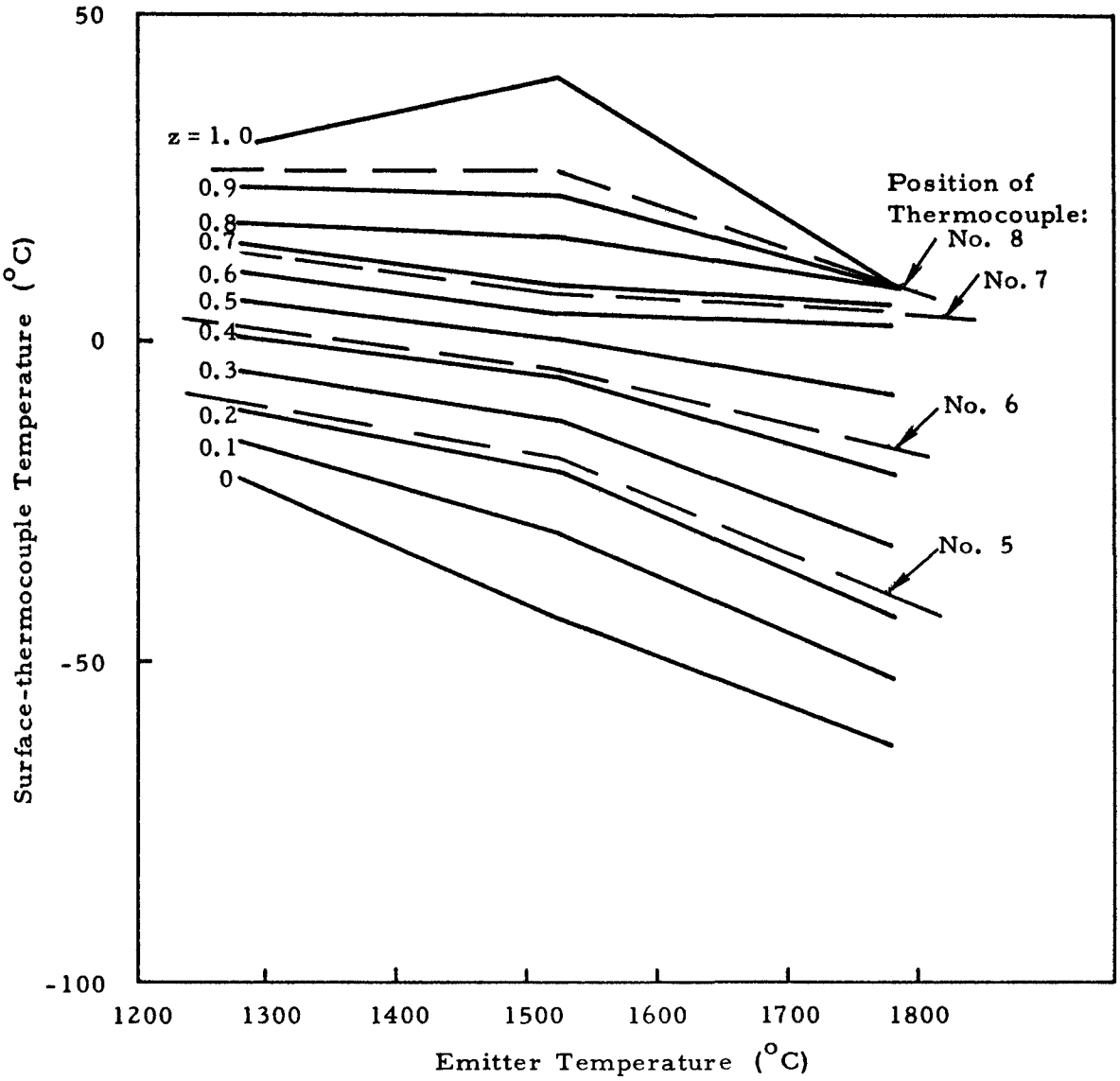

Fig. A-6--OC-4 emitter correlation of thermocouple and surface temperatures

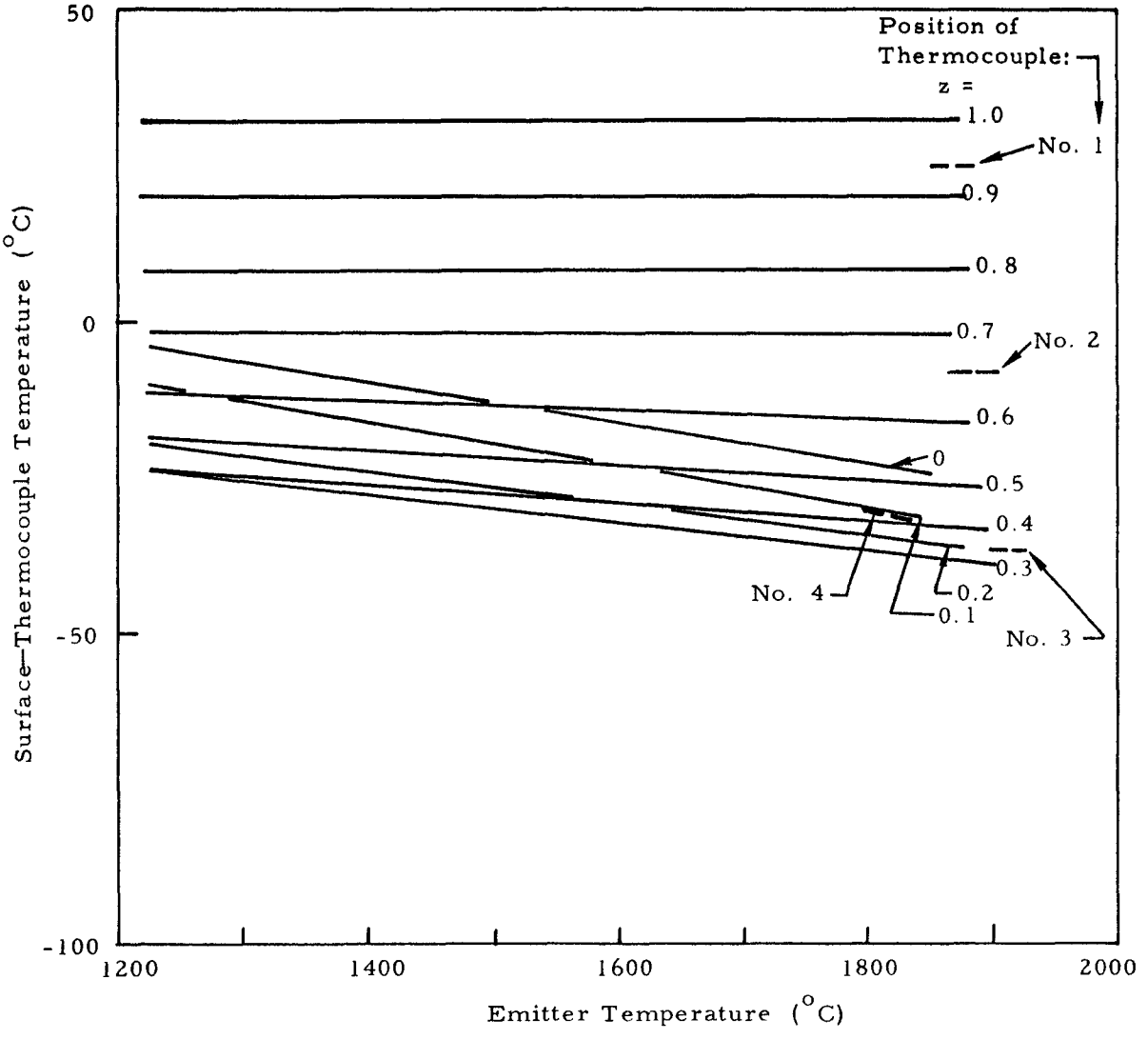

Fig. A-7--OC-5 emitter correlation of thermocouple and surface temperatures

Appendix B

COLLECTOR CALORIMETER CALIBRATION EXPERIMENT

An accurate calorimetry of the energy transferred to the internal surface of the collector is required in order to experimentally obtain an energy balance for a thermionic converter (see Sec. V). The calorimetry method selected for this application uses measured temperature gradients over a known geometry and material to calculate the rate of heat transfer.

A diagram of this "conduction-type" calorimeter is shown in Fig. 1 (Sec. II). The calorimeter consists of a 3-in.-OD by 1.1-in.-long cylinder with a tapered 1-in.-diameter hole in its center. The calorimeter length corresponds to the emitter length. Sixteen stainless steel tubes are brazed into the outer edge of the cylinder for air coolant. Between the tubes are electrical heaters. On each axial end of the cylinder, ten radiation shields are provided to reduce the end heat losses to less than 1 w at the normal operating temperature of less than 700°C. This is about 0.1% of the heat flow to the collector at a maximum power production for an emitter temperature of 1800°C. Twelve calibrated, 40-mil-diameter, sheathed Chromel-Alumel thermocouples are inserted into holes in the calorimeter for measuring the radial, axial, and circumferential temperature distributions. Eight of these thermocouples are used for determining radial temperature gradients.

In the calibration of the collector calorimeter, a filament is suspended into the central cavity of the calorimeter and is used for electron-bombarding the calorimeter inner surface. The ends of the cavity are covered with radiation shields that are electrically insulated from the calorimeter. Figure B-1 schematically shows the calibration set-up and the heat-transfer values of interest in evaluating the calibration results. An energy balance

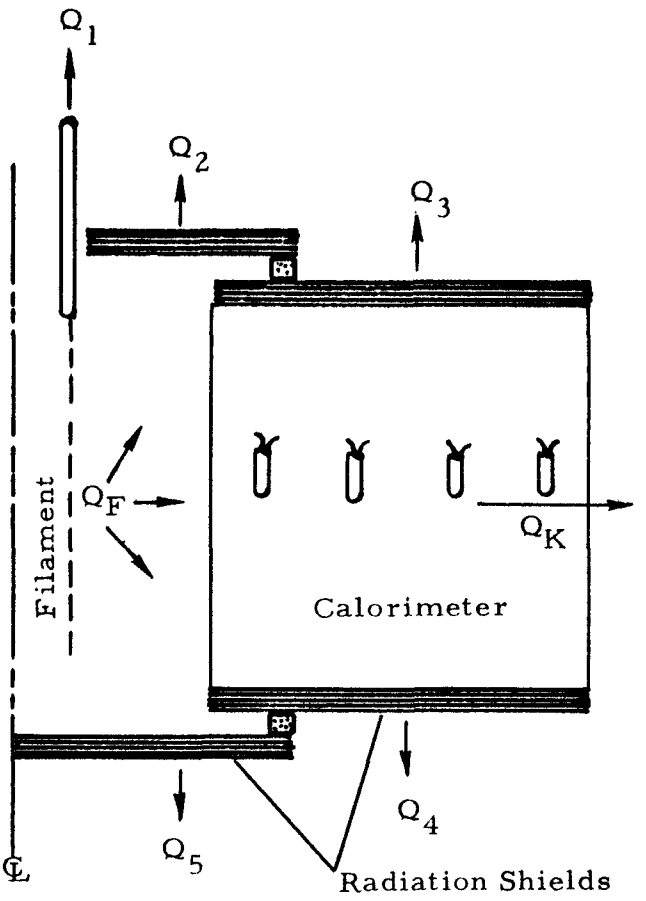

Fig. B-1--Calorimeter calibration energy-transfer quantities

for the apparatus is given by the equation

$$Q_F = Q_L + Q_K , \tag{B.1}$$

where the losses

$$Q_L = Q_1 + Q_2 + Q_3 + Q_4 + Q_5 . \tag{B.2}$$

Q_L was evaluated in two different ways for OC-4 and OC-5. Since no energy data is presented for OC-4 in this report, only the OC-5 calorimeter calibration is described.

Values of Q_L were computed with a two-dimensional, digital-computer heat-transfer code; the maximum computed value was 20 watts. A maximum error in Q_L was estimated to be ±20 watts. With Q_F experimentally determined at accuracies of ±10 watts, Q_K is calculated from Eq. (B.1) with an error of ±22 watts by propagation of the Q_L and Q_F errors.

The radial heat flow through the calorimeter is calculated from the temperature gradients measured with 12 thermocouple combinations by means of Eq. (B.3):

$$Q_{Kij} = \frac{k\, 2\pi\, L(T_i - T_j)}{\ln(r_j/r_i)} , \tag{B.3}$$

where k = thermal conductivity (function of temperature),

L = length of cylinder,

T = temperature,

r = radius,

and i and j are radial thermocouple positions. The experimental procedure for the calibration of the thermocouple pairs is designed to determine if the air cooling or the electrical heating of the outer edge of the calorimeter affects the heat-flow quantities calculated from the radial temperature profiles. To meet this objective, temperature-gradient data are obtained as a function of the electrical power to the filament and of the temperature of the calorimeter.

Out of the 12 possible thermocouple pairs, one pair, designated 2-8, was selected on the basis that the lowest standard deviation determined from multiple measurements was ±25 watts. Figure B-2 shows values of Q_K as a function of $Q_{K2,8}$. The best curve through the points forms the required correlation from which values of Q_K will be calculated from the thermocouple temperatures of thermocouple No. 2 and thermocouple No. 8.

When the calorimeter is used to measure heat from the collector, the filament is removed from the inner cavity and the collector is put in its place. Besides the heat which goes to the calorimeter, other heats which must be accounted for are the heats conducted away from the collector by the collector skirts. This heat transfer is determined by thermocouples spot-welded to the collector skirts at known distances apart. The heat conduction through the top and bottom skirts, Q_{TS} and Q_{BS}, respectively, is computed using the usual conduction equations. The heat-transfer rates are small, and thus the errors inherent in this method of determining the heat flow are unimportant to the over-all accuracy of the calorimetry.

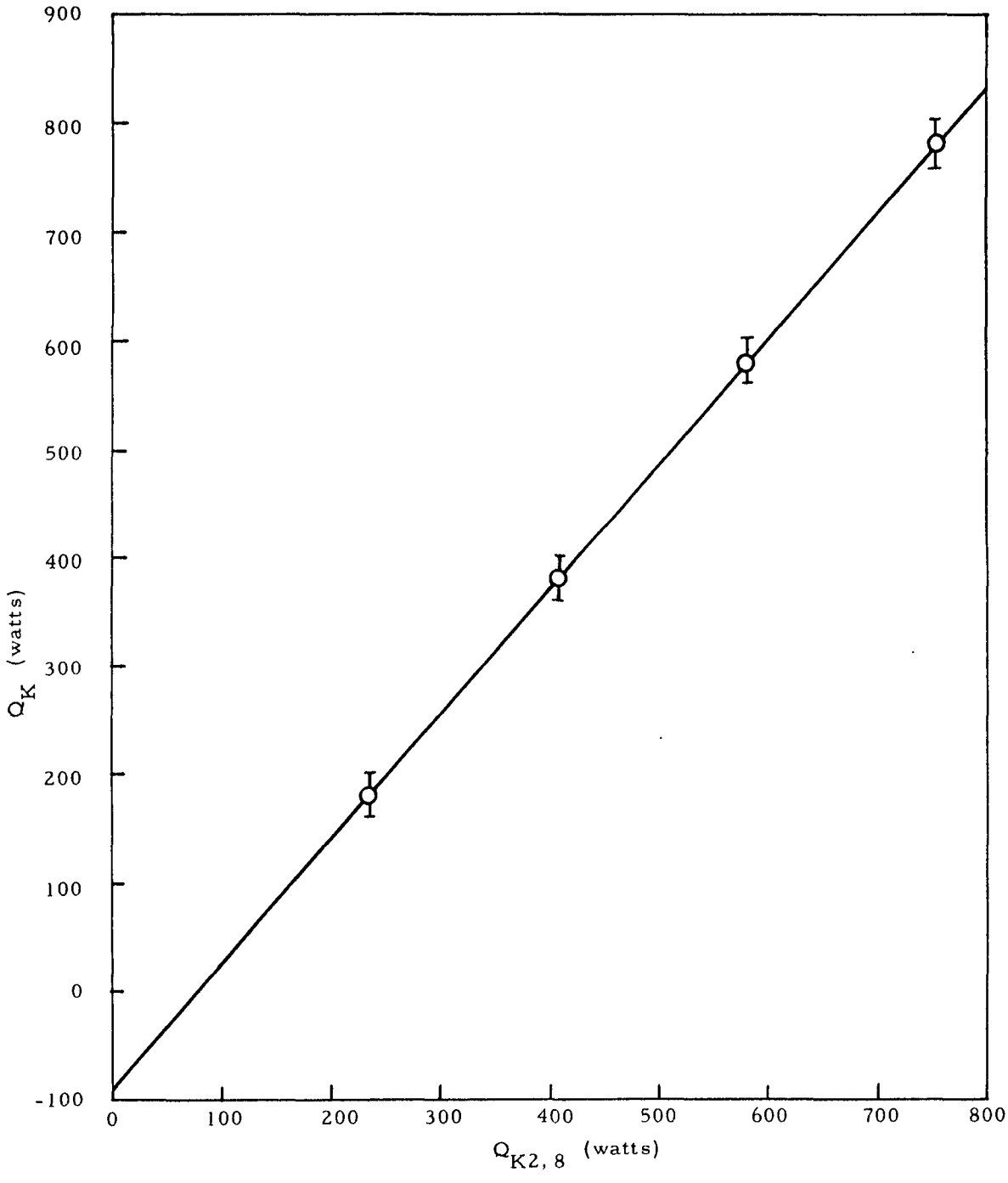

Fig. B-2--OC-5 collector calorimeter calibration

Appendix C

CONVERTER TESTING PROCEDURES

The procedure for testing OC-4 and OC-5 is given in the following outline. Briefly, the procedure consists of (1) obtaining initial maximum performance data early in cell life, (2) performing a detailed performance mapping of the converter operating variables, (3) obtaining converter energy-balance data, and (4) life-testing to a total operating time of 1000 hr.

A. START-UP

1. Operating Conditions
   a. Open-circuit load
   b. Cesium-reservoir temperature $<100^{\circ}C$
2. Measurements and Calculations
   a. Obtain T_E versus Q_E and Q_C data for T_E up to $1800^{\circ}C$* in increments of $100^{\circ}C$.
   b. Show that heat radiated to the collector follows thermal radiation laws.
   c. Compute the effective emissivity of the electrodes as a function of T_E from the heat radiated to the collector.

B. INITIAL PERFORMANCE DETERMINATION

1. Objectives
   a. Obtain initial performance levels early in converter life (within 1/2 hr after $(T_E)_{max}$ is reached).
   b. Obtain initial diagnostic data.
   c. Set the variable boundaries.

*Temperatures refer to the maximum emitter temperature of the distribution. The maximum occurs very near the surface center position.

2. Data

   a. These data are taken immediately following the initial effective emissivity measurements, when the emitter is at 1800°C and the cesium-reservoir temperature is 100°C.

   b. The load is at a low resistance value of about 1 to 2 mohm. Sixty-cycle a-c oscillations of the converter voltage are provided in order for I-V curves to be displayed on an oscilloscope.

   c. (1) The cesium-reservoir temperature is increased by increments to the optimum* value for maximum power output found for previous converters (about 350°C).

   (2) On the approach to 350°C, the temperature is leveled off at 100°, 50°, 25°, and 0°C below the assumed optimum in order to take photographs of I-V curves and to record the cell data at each point.

   d. The sweep circuit is turned off (care being taken not to exceed $(T_E)_{max}$), and the load is adjusted to an approximately optimum condition.

   e. The cesium-reservoir temperature is roughly optimized at $T_E = 1800°C$.

   f. The load is roughly re-optimized by plotting an I-V characteristic at $T_E = 1800°C$.

   g. The collector temperature is roughly optimized at $T_E = 1800°C$, optimum voltage and T_{Cs}.

   h. Steps e, f, and g are reiterated to obtain improved optimum values.

   i. A detailed I-V curve is obtained from short to open circuit at

   $T_E = 1800°C$

   T_C = optimum

   T_{Cs} = optimum

---

*Optimum will always refer to the values of the converter variables which maximize power output.

j. A P versus T_{Cs} curve is obtained at $T_E = 1800^{\circ}C$ and
I = optimum
T_C = optimum

k. A P versus T_C curve is obtained at $T_E = 1800^{\circ}C$ and
I = optimum
T_{Cs} = optimum

3. Computations

a. The variable limits of interest are determined from the above data and from systems-analysis requirements. This will set the limits on the variables investigated in the detailed performance mapping.

b. Any necessary calculations are performed to determine if the cell is performing typically by comparison with previous converters.

C. DETAILED PERFORMANCE MAPPING

1. Objective

Performance mapping of the converter variables:

a. T_E
b. Q_E
c. Q_C
d. T_C
e. T_{Cs}
f. J
g. V

2. Requirements

a. Performance self-consistency is determined regularly by establishing check points twice daily.

b. Data are to be obtained in the easiest but most accurate method available to the investigator. The method will usually be dictated by the available instrumentation. It will be assumed

in the following description that it is easy to regulate T_E, T_C, T_{Cs}, and J. These will be the regulated variables. Q and V will be dependent and nonregulated.

3. Data

   a. Using the variable limits found in B. 3. a. above, a matrix is established involving J, T_C, and T_{Cs}. The matrix spaces are to be filled with V versus T_E and V versus Q data. The matrix mesh points should be closely enough spaced to allow accurate interpolation. It has been found that increments of 1 to 2 amp/cm^2 for J, 5° to 10°C for T_{Cs}, and 50° to 100°C for T_C sufficed.

D. LIFE TESTING

1. The converter is to be operated for 1000 hr at $T_E = 1800^\circ$C.
2. Performance data are obtained daily and plotted to determine trends.

Appendix D

HISTORY OF CONVERTER OPERATIONS

1. OUT-OF-PILE CONVERTER OC-4

The Mark VI out-of-pile converter OC-4 was operated for 1351 hr with an electrical output at the leads of between 3.9 and 5.4 w/cm^2 at a mean emitter temperature of 1750°C. A time history of the operation is shown in Fig. D-1. During the first hours of intermittent operation, start-up and initial performance measurements were obtained which indicated a peak power output of 80 w (5.4 w/cm^2) at an emitter maximum temperature of 1800°C. The mean emitter temperature was estimated at 1750°C from the emitter temperature profile data. A curve of the power at the electrodes (without the I^2R emitter lead loss) is also shown in Fig. D-1; this power density varied between 4.6 and 6.9 w/cm^2.

An accidental excursion in emitter temperature to 2300°C for a few minutes occurred at 22 hr, with a resultant sharp decrease in power density from 5.4 w/cm^2 to 4.9 w/cm^2. Following the excursion, the converter was checked out; it was found that there was no apparent physical damage to the cell or the emitter thermocouples other than a decrease in power output by 10%. This degradation is thought to be caused by outgassing of the emitter and stem, with resultant gas buildup, and possibly by surface work-function changes. It was noted that the collector temperature did not increase from its original level during this short time.

After an additional 25 operating hours, the power density increased to 5.0 w/cm^2 and remained constant until 200 hr. From that point, the power density gradually decreased at a constant rate over the next 1150 hr to a value of 3.9 w/cm^2. Between 50 hr and 500 operating hours, performance mapping and energy-balance data were obtained. During that

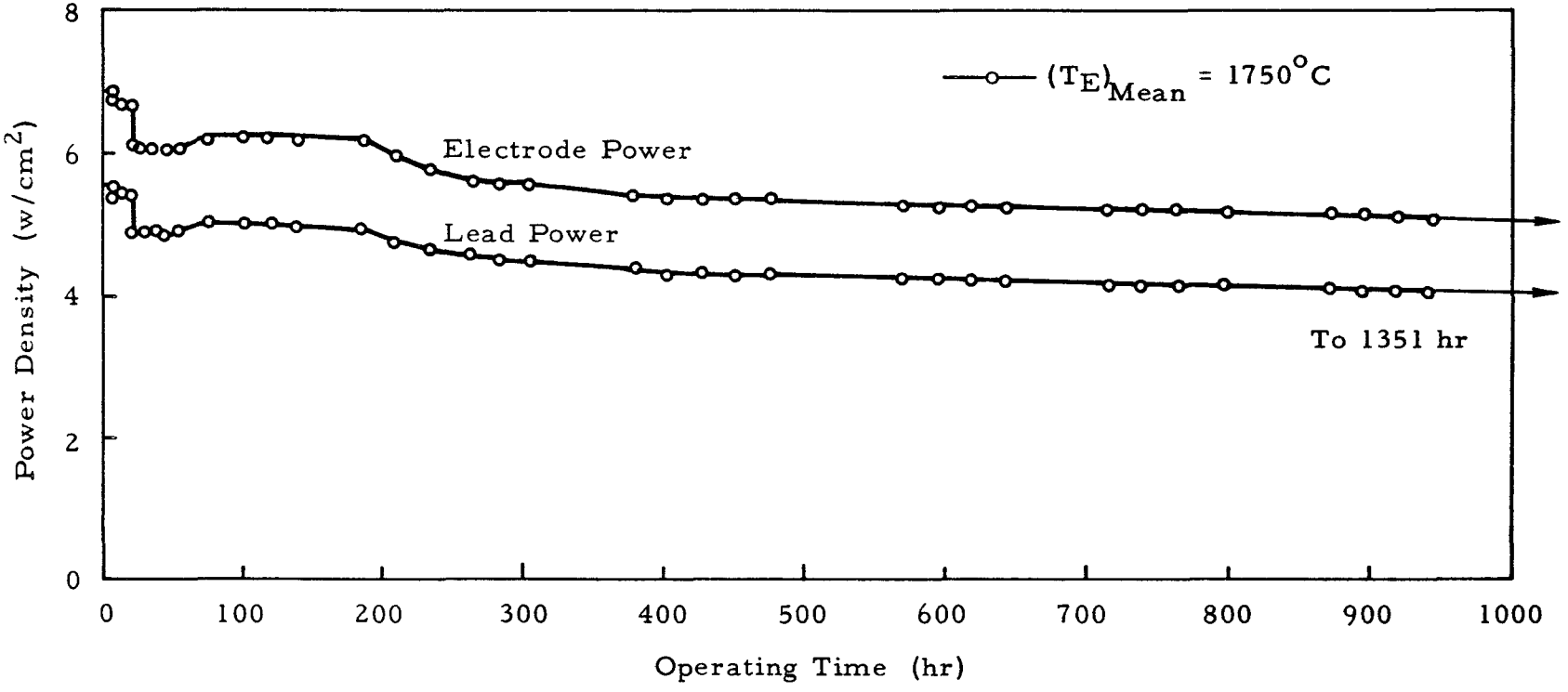

Fig. D-1--Performance history of OC-4 operating at an emitter mean temperature of 1750°C

period of operation, the calorimeter heater open-circuited, and some of the thermocouples on the collector skirts failed. Because of risk to the life-test, it was elected not to make repairs, with the result that no further energy-data or performance mapping was possible. At 1351 hr, a cooling line failed, resulting in an increased bell-jar pressure. The operation was thereupon discontinued.

2. OUT-OF-PILE CONVERTER OC-5

The Mark VI out-of-pile converter OC-5 has operated 260 hr, as shown in Fig. D-2, with a maximum power density of 11.1 w/cm^2 and an efficiency of 16% for a 1800°C emitter mean temperature. Between 100 and 150 hr a gradual performance degradation to 10.5 w/cm^2 was noted. At the end of that period, the source of degradation was found to be a small leak in the calorimeter air-cooling line located inside the bell jar. The effect of this leak was to increase the bell-jar pressure from 1×10^{-6} to 2×10^{-5} torr. Apparently, constituents of air diffused into the cell interior through the high-temperature refractory metal parts to cause the observed degradation. Once the leak was repaired, cell performance degradation immediately ceased; at the end of 260 hr there appeared a perceptible increase in power density to 10.7 w/cm^2. All of the energy-balance and performance-mapping data were obtained during the first 100 operating hours of level performance.

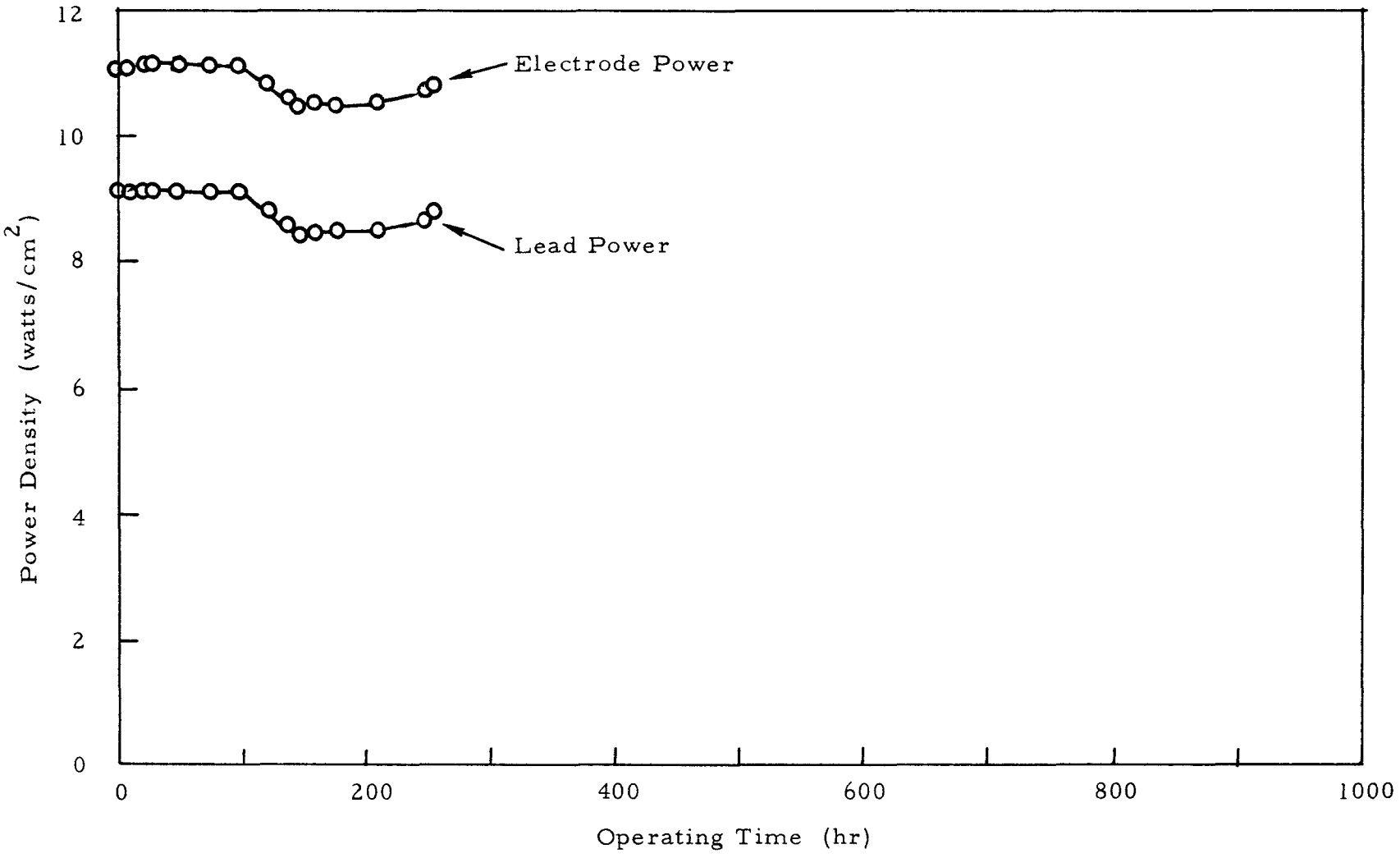

Fig. D-2--Performance history of OC-5 operating at an emitter mean temperature of 1800°C

Appendix E

DATA REDUCTION BY A DIGITAL COMPUTER CODE

The large amount of data, plus the many calibration corrections and correlations involved in each experimental point, make it uneconomical to perform all the data reduction work manually. It was found that each data point required on the order of about 1/2 hr of hand computations to completely reduce the data so that they could be plotted for an interpretation. A digital computer code for thermionic data reduction, TIDR, was written for machine reduction of the data.

The input information on each data point consists of 36 floating-point numbers which correspond to power inputs, power outputs, and thermocouple temperature measurements. The code reduces all of these data and transforms them by means of the various corrections and correlations into a direct output, as shown in Table E-1; an explanation of the symbols in this table is given in Table E-2. It is estimated this code saves several hundred hours of hand-calculation time for each converter tested for performance mapping and energy-balance data. Another advantage is that within several hours after the data are taken, reduced results will be available for interpretation.

In order for the data to be entered directly into the computer library of thermionic data, output cards with the significant data are punched for use with the systems analysis code TIPSY.*

*Broido, J., C. Savery, and W. Wright, A Digital Computer Code for the Analysis of Thermionic Networks, General Atomic Report GA-4147, May 22, 1963.

Table E-1

COMPUTER OUTPUT OF REDUCED OC-4 DATA*

TEMPERATURES			OUTPUT		
EMITTER (MAX)	1785.	C	CURRENT	130.20	A
EMITTER (AVE)	1744.	C	CURRENT DENSITY	8.80	A/CMCM
CESIUM	350.	C	POTENTIAL (LEADS)	0.571	V
COLLECTOR	726.	C	POTENTIAL (ELECT)	0.707	V

POWER OUTPUT			POWER INPUT		
POWER AT LEADS	74.34	W	TOTAL TO EMITTER	872.	W
	5.023	W/CMCM		58.9	W/CMCM
POWER AT ELECT.	92.05	W	TO COLLECTOR	605.	W
	6.220	W/CMCM		40.9	W/CMCM
			COLLECTOR + POWER	697.	W
			AT ELECT	47.1	W/CMCM

OVERALL EFFICIENCY	8.53	PERCENT
ELECTRODE EFFICIENCY	13.20	PERCENT
PHI (RICHARDSON)	3.10	EV

MISCELLANEOUS INPUT AND CALCULATED VALUES.

TE5	1763.	C	TC1	695.	C	TC7	645.	C
TE6	1785.	C	TC2	350.	C	TC11	727.	C
TE7	1734.	C	TC3	589.	C	TC12	736.	C
TE8	1696.	C	TC6	734.	C	TC16	716.	C
ACV	9.22	V	LEAD VOLT	0.136	V	QK	608.3	W
ACA	15.05	A	LEAD RES.	0.001045	OHM	QTS	0.9	W
DCV	470.	V	LEAD I*IR	17.7	WATT	QBS	-4.1	W
DCA	1.56	A	LEAD RHO	0.000056	OHM CM			
			LEAD TEMP.	1195.	C			

DATE8/9/63 TIME1025

I-V AT TEMAXNOM=1800 C TCS=350 C 76

*See Table E-2 for nomenclature.

Table E-2

NOMENCLATURE FOR TABLE E-1

$$\text{OVERALL EFFICIENCY} = \left(\frac{\text{Power Output at Leads}}{\text{Total Power Input to Filament Chamber}}\right)$$

$$\text{ELECTRODE EFFICIENCY} = \left(\frac{\text{Power Output at Electrodes}}{\text{Power Input to the Collector + Power at the Electrodes}}\right)$$

$$\text{PHI (RICHARDSON)} = kT \ln(J/AT^2)$$

$$= (\text{Boltzmann Constant})(\text{Average Emitter Temperature}) \times$$

$$\times \ln[(\text{Current/Emitter Area}) / (\text{Emitter Temp.})^2]$$

TE5 = Emitter Surface Temperature at z = 0.22 in.

TE6 = Emitter Surface Temperature at z = 0.43 in.

TE7 = Emitter Surface Temperature at z = 0.68 in.

TE8 = Emitter Surface Temperature at z = 0.93 in.

TC1 = Emitter Lead Temperature

TC2 = Cesium Reservoir Temperature

TC3 = Calorimeter Temperature at r = 1.27 in.

TC6 = Collector Top Skirt Temperature

TC7 = Calorimeter Temperature at r = 0.55 in.

TC11 = Collector Bottom Skirt Temperature

TC12 = Collector Top Skirt Temperature

TC16 = Collector Bottom Skirt Temperature

ACV = Filament AC Amperes

ACA = Filament AC Voltage

DCV = Bombardment Voltage

DCA = Bombardment Current

Q_K = Heat Conduction in Calorimeter

Q_{TS} = Heat Conduction in Collector Top Skirt

Q_{BS} = Heat Conduction in Collector Bottom Skirt

Appendix F
INSTRUMENTATION

The instrumentation shown schematically in Fig. F-1 was used for bench testing of the Mark VI converters OC-4 and OC-5. The main features of the instrumentation include (1) temperature measurement and control; (2) power output measurement and regulation; and (3) emitter power input supply, control, and measurement.

TEMPERATURE MEASUREMENT AND CONTROL

The emitter temperature was measured with four W/W–26 Re thermocouples located in the emitter walls at four different axial positions. With that arrangement, the emitter temperature level and distribution can be measured during the operations. These thermocouples were calibrated to an absolute accuracy of $\pm 10^{\circ}$C. The relative error is within $\pm 5^{\circ}$C between 1200° and 1800°C. The thermocouple emf was displayed on a zero to 50 mv Brown recorder. The recorder error is ±0.25%.

The temperatures of the calorimeter collector, cesium reservoir, etc., were measured by floating, shielded-type Chromel-Alumel thermocouples. Close regulation of the cesium reservoir and collector was accomplished with a current-adjusting-type three-action proportional controller-recorder. The reservoir and collector temperature errors are estimated to be $\pm 2^{\circ}$C and $\pm 10^{\circ}$C, respectively. The other 20 converter temperatures were intermittently recorded on a 24-point Brown recorder which is accurate within 0.25%.

POWER OUTPUT MEASUREMENT AND REGULATION

The test-cell voltage output was regulated by a high-current variable resistor (load) with a range of 0.001 ohm to 5 ohm. For driving the

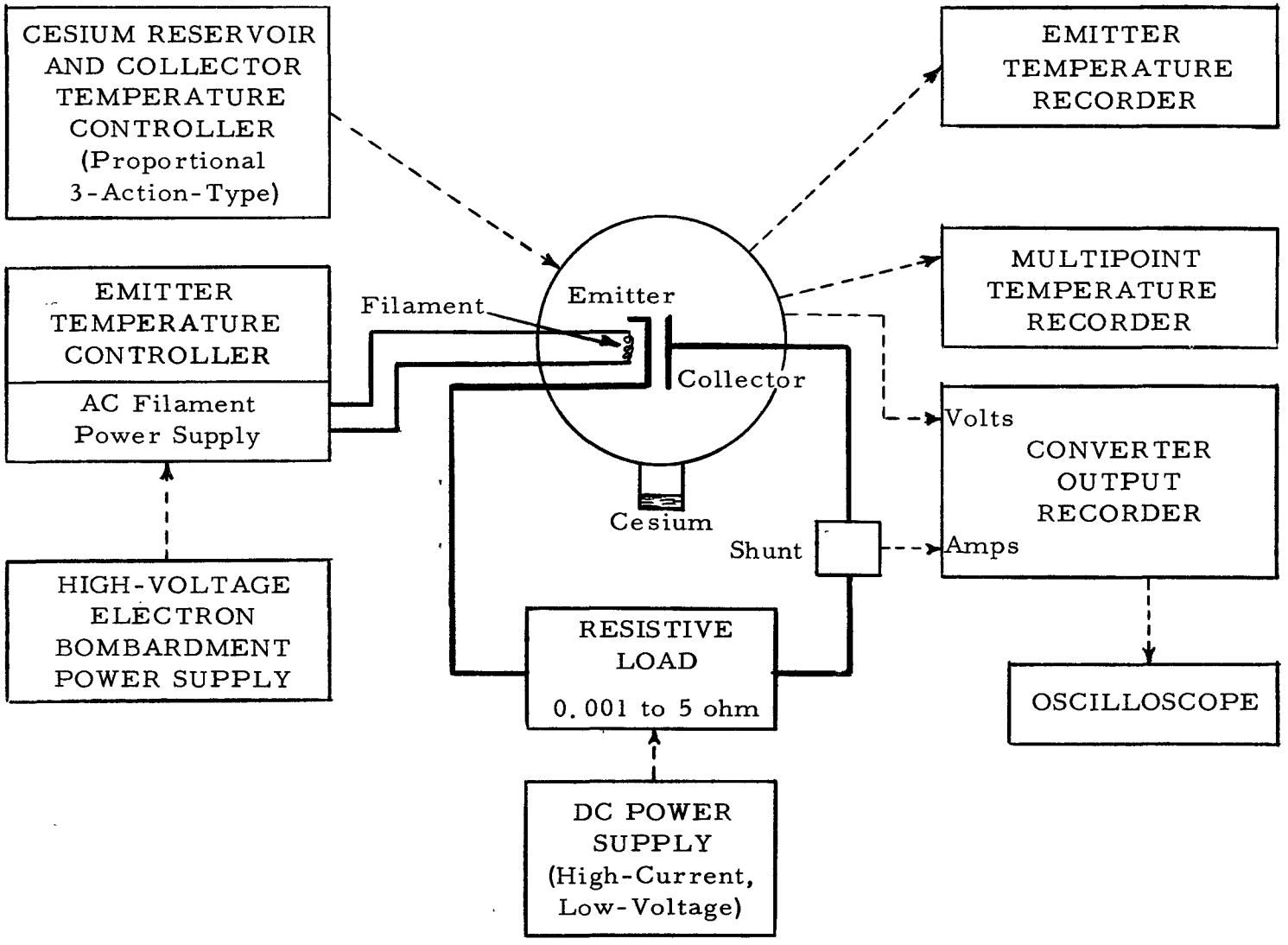

Fig. F-1--Simplified diagram of instrumentation system for bench testing Mark VI converters

test cell into the applied voltage region (+), the parallel battery circuit was used. The driving voltage was regulated with the same resistor.

Converter voltages were measured with copper probes at the emitter, at the emitter lead, and at the collector. The currents were measured with precision shunts. Both the voltage and current were continuously recorded on a Brown two-point recorder. The voltage and current errors are estimated to be ±0.005 volt and ±0.2 amp. A 60-cps voltage sweeping circuit was also used to display voltage-current characteristics on an oscilloscope. Polaroid photographs were used to record the displays.

EMITTER POWER INPUT SUPPLY AND CONTROL

For these bench tests, the emitters were heated artificially by electron bombardment accomplished with a double helical filament suspended in the emitter cavity and supported by 1/16-in. tantalum leads.

The a-c current to the filament is supplied and regulated by a current-adjusting-type three-action proportional controller. The controlled variable is the emitter temperature sensed by one of the W/W–26 Re thermocouples. High voltage was supplied by a regulated d-c power unit with zero to 1000 volt and zero to 5 amp range. The power to the emitter was accurately measured with calibrated precision a-c and d-c meters. The error in the power input measurements is estimated at 1%.